5. Nitrous Oxide and Halocompounds

J.H. BUTLER (EDITOR), J.W. ELKINS, S.A. MONTZKA, T.M. THOMPSON, T.H. SWANSON, A.D. CLARKE, F.L. MOORE, D.F. HURST, P.A. ROMASHKIN, S.A. YVON-LEWIS, J.M. LOBERT, M. DICORLETO, G.S. DUTTON, L.T. LOCK, D.B. KING, R.E. DUNN, E.A. RAY, M. PENDER, P.R. WAMSLEY, AND C.M. VOLK

5.1. CONTINUING PROGRAMS

5.1.1. INTRODUCTION

Research conducted by the Nitrous Oxide and Halocompounds Group (NOAH) of CMDL in 1996 and 1997 included: (1) weekly flask sampling and analysis of air from remote locations and regionally influenced sites, (2) operation of instrumentation for hourly, in situ measurement of trace gases at the four CMDL observatories and at four regionally influenced sites, (3) preparation and maintenance of calibration gases for all measurements, (4) participation on campaigns requiring in situ stratospheric measurements from high-altitude aircraft and balloons, (5) investigation of oceanic processes influencing trace gas composition of the atmosphere, (6) in situ monitoring of air at multiple elevations from tall towers, and (7) measurement of gases in air that is archived in consolidated polar snow in Antarctica and Greenland.

The main mission of NOAH is to measure and to evaluate the distribution and trends of nitrous oxide (N_2O) and many halogenated gases in the atmosphere and ocean with the best analytical tools available. The halogenated gases, or halocompounds, include the chlorofluorocarbons (CFCs), chlorinated solvents (CCl_4, CH_3CCl_3, $CHCl_3$, etc.), hydrochlorofluorocarbons (HCFCs), hydrofluorocarbons (HFCs), methyl halides, halons, and sulfur hexafluoride (SF_6). The recent motivations for measuring these compounds are: (1) that many of the brominated and chlorinated compounds that cause ozone depletion are being phased out of production as required by the amended and adjusted Montreal Protocol [*United Nations Environmental Programme (UNEP)*, 1987, 1997], and (2) that these and many of the compounds introduced to replace them contribute to global warming. The Protocol of the Third Conference of Parties to the United Nations (UN) Framework Convention on Climate Change, held in Kyoto, Japan, December 1997, recommended future limits on the emissions of six compounds or compound groups: (1) carbon dioxide (CO_2), (2) methane (CH_4), (3) nitrous oxide (N_2O), (4) HFCs, (5) SF_6, and (6) the perfluorocarbons (PFC). The last four of these six categories are within the domain of NOAH's research.

Continuing programs within NOAH are based upon in situ or flask air sample measurements from four CMDL observatories and nine cooperative sampling sites (Figure 5.1, Table 5.1. These stations provide a robust network for evaluating global atmospheric change and hemispheric relationships for the various compounds.

One of the more significant discoveries in the past 2 years is the turnover of total anthropogenic chlorine in the atmosphere. This finding came from the combined results of flask sampling, in situ monitoring, and standards programs and is discussed in the following sections.

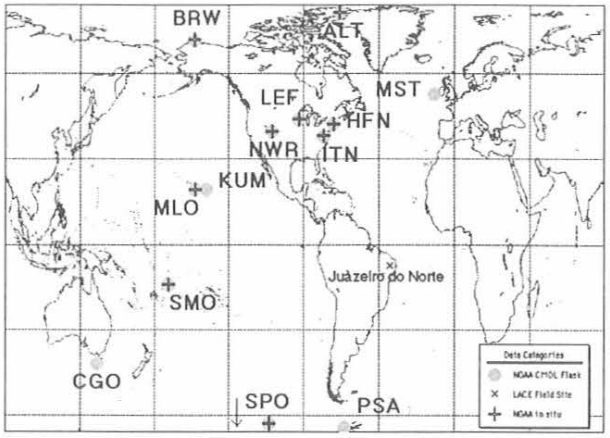

Fig. 5.1. Geographic locations of old and new stations in the NOAH flask (gray circles) and in situ (crosses) networks. The site for the tropical balloon launches, Juazeiro do Norto, Brazil, is noted by an "X."

Other significant results include the observed global increases in atmospheric N_2O and SF_6, again in both flask and in situ monitoring, the continued growth of atmospheric HCFCs and HFCs as they increasingly are used as replacements for the ozone-depleting CFCs, and the surprising, protracted growth of the halons in the atmosphere years after the cessation of their production in developed countries.

5.1.2. FLASK SAMPLES

Overview

The flask sampling program has undergone a few changes in 1996-1997 designed mainly to facilitate processing of samples and data. Over the past decade the number of gases analyzed by this group has risen from 3 to over 25 and the number of weekly sampling sites has more than doubled, from 5 to 11 (Figure 5.1, Table 5.1). Additional flasks are collected as part of special projects, including oceanic expeditions, polar firn sampling, and aircraft missions. Flasks that once were analyzed by one instrument are now analyzed by four instruments, two of which are mass spectrometers (Table 5.2). This increase in the number of flasks sampled and gases measured has resulted in a considerable increase in the laboratory workload. Attempts to offset this have focused on automation of instruments, streamlining of data processing, and improvement of quality control. In 1991 the first of the automated instruments, a three-channel gas chromatograph (GC) electron capture detector (ECD) system capable of measuring seven gases, was put in service. This system replaced the old manual, one-channel

TABLE 5.1. Geographic and Network Information on NOAH Network Sites

Code	Station	Latitude	Longitude	Elevations (m)	LST-GMT (hr)	Type
ALT	Alert, Northwest Territories, Canada (AES)*	82.45°N	62.52°W	210	-4	F, I
BRW	Point Barrow, Alaska	71.32°N	136.60°W	11	-9	F, I
MHT	Mace Head, Ireland (University College)	53.33°N	9.90°W	26	0	F
LEF	WLEF tower, Wisconsin (CMDL-CCG)	45.95°N	90.28°W	470	-6	F, I
HFM	Harvard Forest, Massachusetts (Harvard University)	42.54°N	72.18°W	340	-5	F, I
NWR	Niwot Ridge, Colorado (University of Colorado)	40.04°N	105.54°W	3013	-7	F, I
ITN	WITN tower, North Carolina (CMDL-CCG)	35.37°N	77.39°W	9	-5	F, I
MLO	Mauna Loa, Hawaii	19.54°N	155.58°W	3397	-10	F, I
KUM	Cape Kumukahi, Hawaii	19.52°N	154.82°W	3	-10	F
SMO	Tuluila, American Samoa	14.23°S	170.56°W	77	-11	F, I
CGO	Cape Grim, Tasmania, Australia†	40.41°S	144.64°E	94	+10	F
PSA	Palmer Station, Antarctica‡	64.92°S	64.00°W	10	+12	F
SPO	South Pole, Antarctica	89.98°S	102.00°E	2841	+12	F, I

Cooperative sites (F = flasks, I = in situ) with:
*In situ GC: Only N_2O and SF_6; flask sampling for all gases, however.
†Commonwealth Scientific and Industrial Research Organization (CSIRO) and Bureau of Meteorology, Australia
‡Only glass flasks used.

GC/ECD that measured only three gases [*Thompson et al.*, 1985]. After a few years of debugging and intercomparison, the old, manual GC/ECD was retired in 1996. Software for running the automated GC/ECD system was upgraded in 1995. In the past 2 years quality control programs were written and a database developed that now allows evaluation of data from samples immediately following analysis.

TABLE 5.2. Instrumentation for NOAH Flask Analysis

Instrument	Type	Gases	Frequency of Network Data
OTTO	GC/ECD, 3-channel, isothermal	N_2O, CFC's (3) ClC's (2) SF_6	Weekly
LEAPS	GC/ECD, 1-channel, temperature programmed	Halons (2) CH_3Cl CH_3Br CFC's (1)	Semi-monthly to monthly
HCFC-MS	GC/MS, 1-channel, temperature programmed	HCFCs (3) HFCs (1) CFCs (3) Halons (1) ClCs (6) BrCs (3)	Semi-monthly
HFC-MS	GC/MS, 1-channel, temperature programmed	HCFCs (5) HFCs (2) CFCs (2) Halons (2) ClCs (6) BrCs (3) ClBrCs (3)	Semi-monthly to monthly

Other efforts at automation included the GC mass spectrometer (MS) mainly responsible for measurement of HCFC's and methyl halides, and an additional GC electron capture detector (ECD) system, Low Electron Attachment Potential Species (LEAPS), mainly used for measurement of halons and methyl bromide. Programs also have been written to speed up processing of data from these instruments. Peak integration is now fully automated on both GC/MS instruments, although manual integration of peaks is still necessary on the LEAPS GC/ECD system.

Thirty-two new, 3-L sampling flasks from Meriter Corporation (San Jose, California) were purchased for inclusion in our sampling network. These flasks are constructed from no. 316 stainless steel, are highly electropolished, and have minimal internal weld exposure. Stability is excellent for most gases in these flasks, although CCl_4 and, to a lesser extent, CH_3CCl_3 can degrade over the long term as they do in all stainless steel flasks filled with dry air. Recent work with glass flasks in sampling firn air has shown that glass flasks identical to those used in the carbon cycle network can be used for sampling halocarbons over the short term. Further tests of flasks already in the network showed that many of them, depending upon their history, can be contaminated. We continue to purchase and test these in small lots as a possible option for use in special projects and for measuring gases that are less stable in selected stainless steel flasks.

A number of improvements at our flask sampling sites during 1996 and 1997 were made. At SMO the sample inlet was moved from the stack to the pump board Air-Cadet inlet system of the Radiatively Important Trace Species (RITS) GC to avoid cross contamination from other observatory instruments with inlets attached to the stack. Samples are now collected from the continuous flow, pressurized inlet at all sites except CGO, which will be changed over in 1998. Because of concerns about the durability of the Air-Cadet pumps for use with the RITS

inlet system and flask sampling, existing pumps were replaced with KNF Neuberger N-05 pumps during visits to the South Pole Observatory, Antarctica (SPO), Mauna Loa Observatory, Hawaii (MLO), Cape Kumukahi, Hawaii (KUM), and SMO. Pumps at the remaining sites will be upgraded in 1998. At KUM before November 1997, a pump system was connected upstream of the continuously flowing, Air Cadet pump to facilitate flask sampling. In November 1997 the Air cadet pump was replaced by a continuously flowing KNF Neuberger pump. Flasks can now be sampled from a simple manifold. BRW and CGO will be visited in 1998 to receive the same improvements. At NWR, AC power was installed at T-van. The battery-powered pump system will be replaced by a new system that allows flasks to be filled to higher pressures.

In addition to improvements at these sites, sampling with glass flasks was initiated at Palmer Station, Antarctica (PSA) at the end of 1997 in an attempt to understand the seasonal cycling of some of the more reactive halogens at a southern hemispheric coastal site. The objective is to compare results from this site with those from BRW where seasonal cycles are pronounced and perhaps influenced by the springtime breakup of ice. With assistance from CMDL's Carbon Cycle Group (CCG), samples are collected in glass flasks two times per month. The glass flasks are filled to about 1.3 kPa with the CCG MAKS sampling apparatus by personnel trained by CCG. Although contamination is observed for some halocarbons, pump tests and preliminary results suggest good data can be obtained for many other compounds with this technique.

CFCs and Chlorocarbons

Measurements from the automated flask GC (OTTO) show that atmospheric mixing ratios of CFC-11 and CFC-113 continued to decline through 1996 and 1997 at rates similar to those previously reported for earlier years [*Montzka et al.*, 1996], while the growth rate of CFC-12, although still positive, decreased from 5.9 to around 4 ppt yr^{-1} (see cover figure). As a result of declining concentrations and growth rates for CFCs, methyl chloroform, and CCl_4, the amount of chlorine, equivalent chlorine (chlorine + bromine weighted by an efficiency factor), and effective equivalent chlorine (equivalent chlorine weighted by destruction rates in the midlatitude stratosphere) contained within long-lived, halogenated gases (CFCs, HCFCs, CH_3CCl_3, CCl_4, and halons), peaked in 1992-1994 and declined through 1995 [*Montzka et al.*, 1996]. *Cunnold et al.* [1997] found similar results for chlorine-containing compounds measured by the Advanced Global Atmospheric Gases Experiment (AGAGE). The measurements suggest that declines in these quantities continued during 1996-1997 at rates similar to those observed in mid-1995 (Figure 5.2). Amounts observed at the end of 1997 represent a decrease of 2-4% from the peak Cl, ECl, and EECl delivered to the atmosphere from these gases in earlier years. Relative declines in the total atmospheric burden of Cl, ECl, and EECl are smaller because other gases (e.g., CH_3Cl and CH_3Br) also contribute significantly to the atmospheric burden of these quantities.

The gas contributing the most to this decline is CH_3CCl_3, which has an atmospheric lifetime of less than 5 years. As this gas is removed from the atmosphere, the overall rate of the decline in total chlorine will become slower. However, distributions and trends of this gas allow understanding of other atmospheric processes. For example, the difference in the atmospheric mixing ratio of CH_3CCl_3 between hemispheres has become dramatically smaller since 1992 as emissions have declined. The global latitudinal distribution of CH_3CCl_3 in 1992 and earlier years reflected the distribution of sources; mixing ratios in the northern hemisphere were higher than in the southern

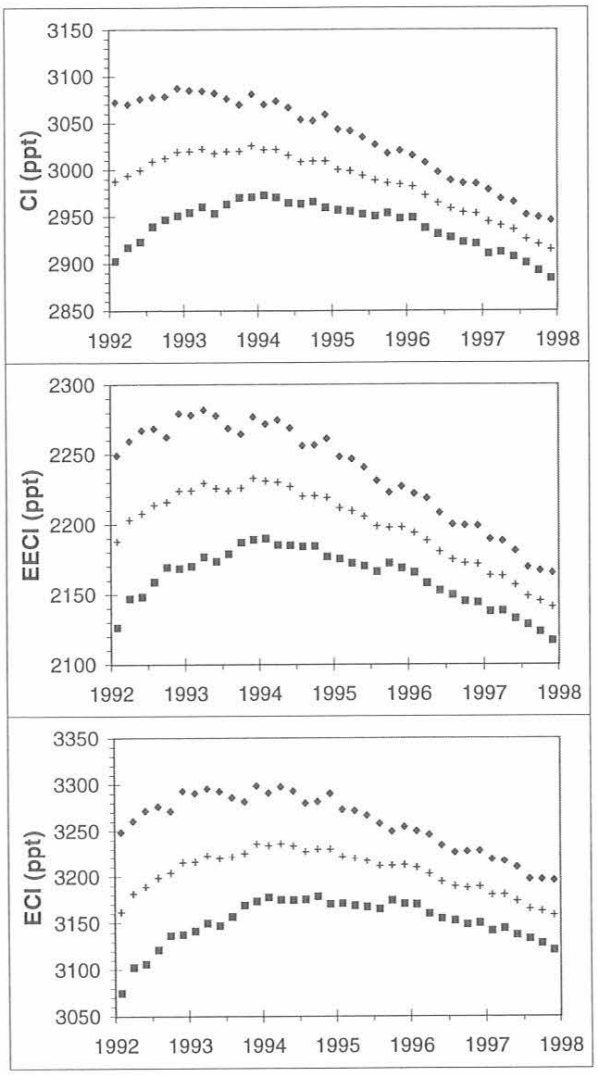

Fig. 5.2. Trends in chlorine, equivalent chlorine (chlorine + bromine multiplied by an efficiency factor of 50), and effective equivalent chlorine (equivalent chlorine where compound-specific halogen release rates are considered) from CFCs, HCFCs, halons, CCl_4, and CH_3CCl_3. Symbols refer to the northern hemisphere (filled diamonds), southern hemisphere (filled squares), and global tropospheric mean (crosses).

hemisphere because this solvent was emitted predominantly in the northern hemisphere. As emissions become insignificant, the distribution of CH_3CCl_3 will instead reflect the latitudinal distribution of sinks for this compound, which is dominated by the reaction of CH_3CCl_3 with the hydroxyl radical (Figure 5.3). Since the summer of 1996, mixing ratios at SMO have been lower than at CGO, likely as a result of the greater abundance of OH in the tropics. Continued monitoring of methyl chloroform as emissions diminish further should allow for refined estimates of the global lifetime of CH_3CCl_3 and, therefore, of other trace gases that react with OH. It also will be useful in estimating the relative mean OH abundance in the northern and southern hemispheres.

The global mixing ratio of CCl_4 is more difficult to determine from flask samples because CCl_4 (and to a much lesser extent CH_3CCl_3 and CH_3Br) can be degraded in dry air samples stored for extended periods in stainless steel flasks. This is indicated by anomalously low mixing ratios and poor flask pair agreement in many of the samples collected at SPO and less frequently from wintertime samples collected at ALT, BRW, MLO, and NWR. Nevertheless, measurements from reliable flask samples (those for which pair agreement is within acceptable limits) support the trends and abundance determined by the RITS program, showing a continued decrease of 0.8 ppt yr^{-1} for atmospheric CCl_4 through 1996 and 1997.

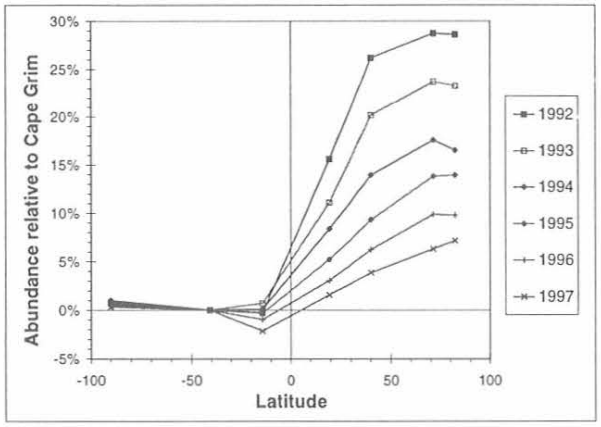

Fig. 5.3. The annual mean abundance of methylchloroform relative to the abundance at Cape Grim, Tasmania, for that year. Similar years are connected with lines to guide the eye. Mixing ratios are determined from GC/MS analysis of paired flask samples.

N_2O

The growth rate of atmospheric N_2O over the past two decades has ranged from under 0.5 to over 1.0 ppt yr^{-1}. The mean, globally-averaged growth rate of this gas from flask measurements during this time was 0.75 ± 0.03 (95% confidence limits (C.L.)) ppt yr^{-1}, which amounts to about 0.25% yr^{-1}. These data and growth rates are from 20 years of flask analyses and are corroborated by measurements with RITS in situ instrumentation over the past 11 years (section 5.1.3). The factors that cause this increase and determine the isotopic composition of atmospheric N_2O are currently unexplained [*Bouwman et al.*, 1995; *Cicerone*, 1989; *Kim and Craig*, 1993]. However, our measurements of firn air [*Battle et al.*, 1996] and other ice-core records [*Khalil and Rasmussen*, 1989; *Leuenberger and Siegenthaler*, 1992; *Machida et al.*, 1995] show clearly that N_2O has been increasing in the atmosphere for at least the past 100 years.

SF_6

SF_6 is a trace gas only recently introduced into the atmosphere. It has a lifetime of ~3200 years [*Ravishankara et al.*, 1993] and a greenhouse warming potential (GWP) of 15,000-35,000 [*Schimel et al.*, 1996], making it an extraordinarily strong greenhouse gas on a per molecule basis. SF_6 is used mainly as an insulator in electrical transformers and circuit breakers. Once leaked into the atmosphere, it will persist for millennia. Although present at low ppt levels in today's atmosphere and currently of little global consequence, SF_6 has been increasing in abundance since the early 1970s [*Geller et al.*, 1997; *Maiss and Levin*, 1994]. SF_6 data, which include archived air samples and recent samples from the flask network, show that the growth rate has not changed much over the past decade (Figure 5.4). The growth rate of 0.20 ± 0.03 (95% C.L.) ppt yr^{-1} from the flask network samples, which run from 1995-1998, does not differ

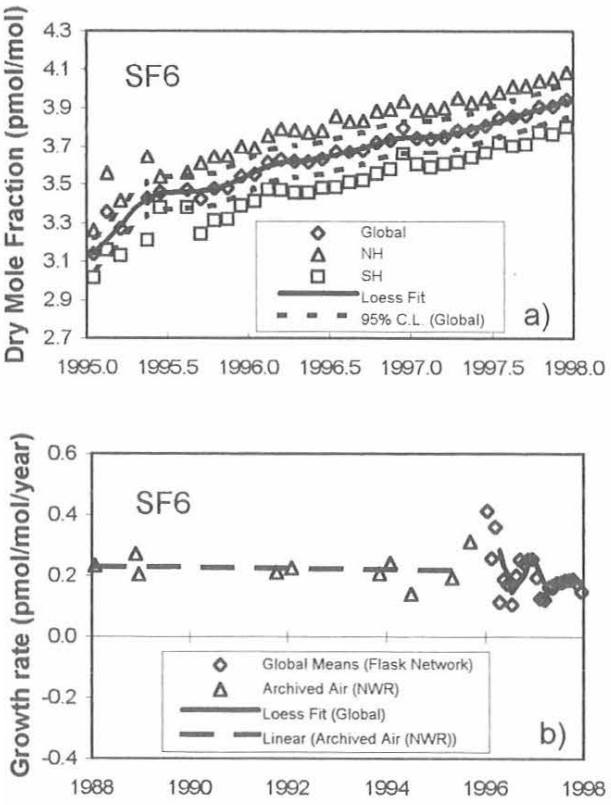

Fig. 5.4. CMDL measurements of atmospheric SF_6. (a) Global and hemispheric averages of the dry mole fraction of SF_6 in flask samples dating back to 1995. (b) Annual growth rates calculated from year-to-year differences in the global mean N_2O. The dark line is a loess smooth of the data.

significantly from the 0.22 ± 0.03 (95% C.L.) ppt yr^{-1} determined from archived NWR samples which go back to 1987. Northern hemisphere (NH), southern hemisphere (SH), and global growth rates for this gas are identical, which is to be expected for a gas with constant source strength and long lifetime.

Halons

Measurements show that the atmospheric burden of halons H-1301 and H-1211 has doubled and that of H-2402 has increased by over half during the past decade (Figure 5.5) [*Butler et al.*, 1998]. Halon mixing ratios continued to increase in recent years despite an international ban on their production and sales in developed nations effective January 1, 1994. The growth rate of H-1301 appears to have slowed recently, but it remains significant (Table 5.3, Figure 5.5a) and, within stated uncertainties, the 1997 growth rate does not differ from that reported for the end of 1996 [*Butler et al.*, 1998]. Atmospheric H-1211 is increasing at a much higher rate than H-1301 and has not shown much sign of slowing over the past decade (Table 5.3, Figure 5.5b). The 1997 tropospheric growth is virtually identical to growth over the past decade. Although the growth rate of H-2402 is substantially slower than that of the other two halons, H-2402 contains two bromine atoms per molecule. Thus the increase of Br due to growth of H-2402 in the atmosphere in 1996 is almost half that of H-1301 and about one-tenth that of H-1211.

Few measurements of halons that allow for accurate comparisons to the results presented here have been reported over the past decade. Usually such reports are associated with field missions that are limited in geographic distribution, period of sampling, or both. Some are part of stratospheric investigations, so contribute only a few values for the troposphere. Even if these differences in sampling are taken into account, it is still clear that measurements from these studies in the past have not agreed well (Figure 5.6). Such widespread disagreement among laboratories underscores the need for extensive intercalibration among investigators making these measurements. Small offsets in calibration can lead to large errors in estimates of potential ozone depletion because of the possibility of the halons offsetting gains in stratospheric ozone protection resulting from reductions in chlorocarbon emissions [*e.g.*, *Montzka et al.*, 1996]. Small errors in estimating the atmospheric burden of halons can lead to significant errors in estimates of the atmospheric burden or trend of equivalent chlorine in the atmosphere [*Daniel et al.* 1996].

Evaluations of the growth rates and the amounts of "banked" halon available for use suggest that H-1301 emissions could continue at the present rate for another 40 years before depleting the bank of H-1301 [*Butler et al.*, 1998]. This would leave an atmospheric mixing ratio of 3.6 ppt, or 57% higher than observed today. Under the same scenario, reserves of H-1211 would be depleted in 8 to 12 years leaving an atmospheric mixing ratio of 4.6-5.0 ppt, or 31-43% higher than observed today. However, there is a significant discrepancy between H-1211 emissions calculated from production and use and emissions deduced from atmospheric measurements. The discrepancy can be reconciled by lowering estimated emissions by ~25%, reducing the atmospheric lifetime of H-1211 from the 20 years given in *Kaye et al.*, [1994] to 11 years or some combination of the two [*Butler et al.*, 1998]. These uncertainties cause considerable doubt in

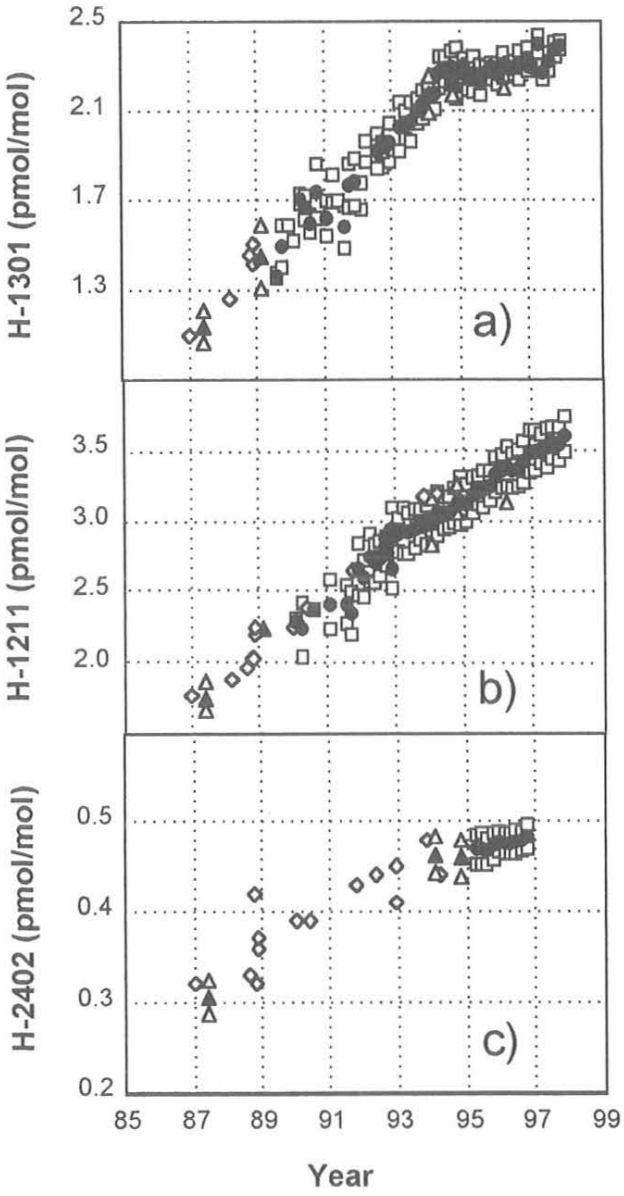

Fig. 5.5. Hemispheric and global bimonthly averages of tropospheric mole fractions of (a) H-1301, (b) H-1211, and (c) H-2402. Data are taken from the CMDL flask network (squares), research cruises (triangles), and cylinders of archived air (diamonds). Northern hemispheric results are shown as shaded symbols, southern hemispheric results as open symbols, and global means as solid symbols. Bimonthly, hemispheric averages are calculated by weighting measurements by the cosine of the sampling latitude within each hemisphere. Global averages are computed as means of the hemispheric averages.

TABLE 5.3. Atmospheric Halons

Gas	Tropospheric Mole Fraction (pmol mol^{-1})	Global Growth Rate (pmol mol^{-1} yr^{-1})
H-1301	2.4 ± 0.1	0.044 ± 0.015
H-1211	3.6 ± 0.1	0.15 ± 0.02
H-2402	0.45 ± 0.03	0.009 ± 0.001

Tropospheric mole fractions for H-1301 and H-1211 are for the end of 1997. The tropospheric mole fraction for H-2402 is for the end of 1996. Global growth rates for H-1301 and H-1211 are given as the observed change in the latitudinally weighted, global, mean mixing ratios for 1995-1997 for H-1211 and for 1995-1996 for H-2402.

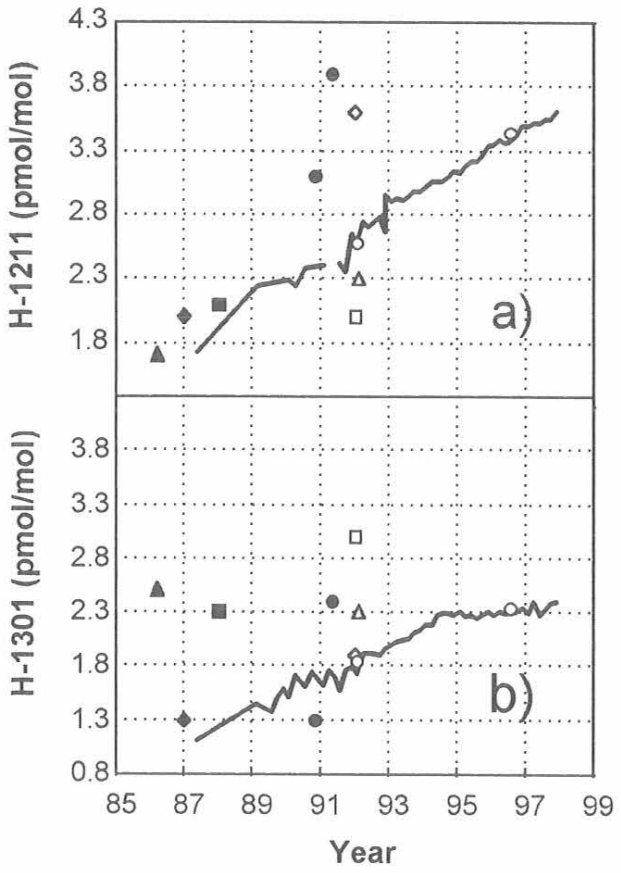

Fig. 5.6. Measurements of tropospheric halons over the past decade. Solid lines are CMDL global averages for (a) H-1211 and (b) H-1301. Symbols signify measurements by other laboratories and research groups. Filled squares represent work by Khalil and Rasmussen [*Ehhalt et al.* 1988, *Khalil and Rasmussen*, 1992], open triangles are from a study by *Singh et al.* [1988], open squares represent measurements by *Oertel* [1992], filled circles are measurements by C.J.-L. Wang, D.R. Blake, N. Blake, and F.S. Rowland, as given in *Lorenzen-Schmidt* [1994], filled diamonds are values from *Lorenzen-Schmidt* [1994], open circles are from *Schauffler et al.* [1993], and filled triangles are from *Fabian et al.* [1994].

modeled predictions of the future burden and fate of H-1211 in the atmosphere. It is not certain whether the continued rapid increase in H-1211 results from a depletion of known reserves, inordinately high fugitive emissions during its production in third world countries, or unreported production of halon.

Chlorofluorocarbon Alternatives Measurement Program (CAMP)

Measurements of chlorofluorocarbon alternatives continued on two instruments during 1996 and 1997. On average, one to three flask pairs per month from eight remote and three regional sampling locations were analyzed on the older GC-MS instrument. In addition, about one sample flask pair per month was analyzed from the remote locations on the instrument dedicated to making measurements of HFC-134a. The main changes made in this program involved automated data manipulation on both instruments as of January 1997 and automated analysis of larger flasks on the older GC-MS instrument as of September 1997.

Automated data manipulation allows results to be calculated and compiled more efficiently. This is achieved through the use of macros that determine chromatographic peak areas and calculate and compile results with a commercially-available spreadsheet software package. Automation allows for unattended analysis of up to eight flasks or four high-pressure cylinders. Flasks and secondary air standards are connected via a 16-port stream selection valve to the instrument inlet. Flows from flasks are regulated with different lengths of small diameter stainless steel tubing that are matched to the initial flask pressures. With automated analysis, agreement between replicate injections and between simultaneously filled flasks is similar to or improved over manual analysis. Results from a subset of flasks analyzed by both methods agreed for nearly all compounds. Some small offsets were observed for HCFC-142b and HCFC-141b and appear to result from problems associated with manual analysis of flasks. Protocols for routine checking of sample integrity as it passes through the multiple sampling ports are being implemented.

Mixing ratios of the most abundant HCFCs (HCFC-22, -141b, and -142b) continue to increase throughout the troposphere (Figure 5.7, Table 5.4). In mid-1997 these three gases accounted for about 5% or 150 ppt of the atmospheric burden of chlorine contained within long-lived, anthropogenic halocarbons. This amount was increasing by about 10 ppt per year in 1997 or similar to that reported for earlier years [*Elkins et al.*, 1996a; *Montzka et al.*, 1996].

Continued increases were also observed for HFC-134a, a gas for which restrictions on future use are being considered as part of the Kyoto Protocol (Figure 5.7, Table 5.4). Global mixing ratios of this CFC replacement are currently below 10 ppt. Because of laboratory air contamination and other issues, the number of good measurements made in 1997 was limited, but improvements are being implemented to avoid these problems in the future.

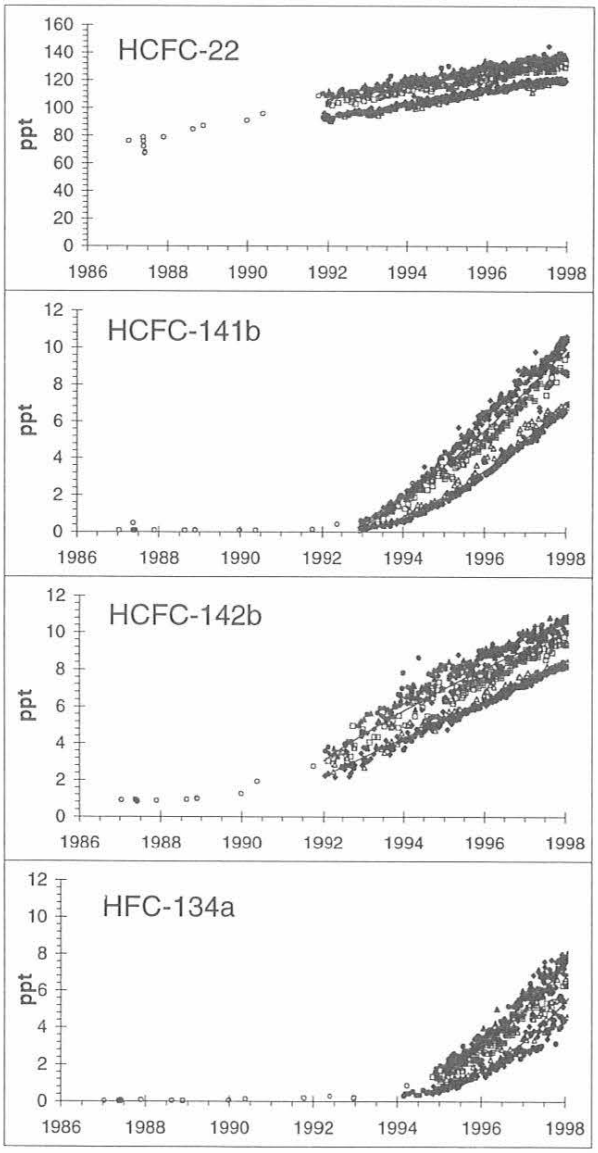

Fig. 5.7. Atmospheric dry mole fractions (ppt) of the most abundant HCFCs and HFC-134a. Each point represents the mean of two simultaneously filled flasks from one of eight stations: ALT, filled circle; BRW, filled triangle; NWR, filled diamond; KUM, crosses; MLO, open square; SMO, open triangle; CGO, filled diamond; SPO, filled circle. Also plotted are results from analysis of archived air samples (open circles) filled at NWR and in a past cruise from both hemispheres (mid-1987).

Short-Lived Gases

Measurements of CH_2Cl_2, $CHCl_3$, and C_2Cl_4 by GC-MS techniques continued from remote flask sampling locations during 1996-1997 (Figure 5.8) and as part of CAMP. Beginning in 1995 the use of a new type of flask built at Max Planck Institute for Chemistry (MPI), Mainz, Germany, allowed for more reliable measurements of CH_2Cl_2 and $CHCl_3$, and reliable measurements of CH_3Cl and CH_3Br (Figure 5.8). These MPI flasks are larger (2.4 L versus 0.8 L), made out of a higher grade stainless steel, and do not contain any seals that require Teflon tape. Results from simultaneously filled pairs of these flasks generally agree to within the instrument measurement capabilities, suggesting that mixing ratios of gases contained within the flasks do not change during storage and transport. This was not true for some gases, particularly CH_3Cl and CH_3Br in the older, 0.8-L flasks.

TABLE 5.4. Global Mid-Year Burden and Rate of Change for HCFCs, and HFC-134a

Compound	Mid-1996 Mixing Ratio (ppt)	Mid-1997 Mixing Ratio (ppt)	1996-1997 Growth Rate (ppt yr^{-1})
HCFC-22	121.6	126.0	4.9*
HCFC-141b	5.4	7.4	1.9
HCFC-142b	7.7	8.7	1.0
HFC-134a	3.1	5.4	2.1

Quantities estimated from latitudinally weighted measurements at seven remote sampling locations.

*Growth rate estimated from 1992-1997.

5.1.3. Radiatively Important Trace Species (RITS) Measurements

Operations Update

The major operational change in this program over the 2-year period of this report was the relocation of equipment to new buildings at three sites. The air line intakes were not moved during this period, but in November 1995 the tower at SPO was moved and the lines extended to accommodate construction of the Atmospheric Research Observatory (ARO). Normal equipment and software maintenance continued as usual based on failures and problems reported by the site personnel.

At the C-1 site on Niwot Ridge, Colorado, a 3 m × 5 m Tall Ranch Tuff Shed was placed at the site in early October 1995 east of the existing facility. Over the next 6 months as time and weather permitted, a window was installed and the interior of the structure was wired for electricity. The building was insulated and wall board, flooring, heating equipment, and air conditioning were installed. Finish work was done by NOAH staff. University of Colorado personnel brought power to the building and installed a fiber optic computer network. On April 3, 1996, all of the equipment was moved into the new building. As the air lines were moved, one of the lines was found to have a small hole in it about 1 m from where it entered the old building. The Dekabon tubing was cut at that point and attached to the pump in the new building. A comparison of the previous month's data shows no significant difference between the two air lines for any of the chemicals measured.

The new building at SMO was completed in early July 1996 and our equipment was the first to be moved from the old EKTO building. The equipment was checked and then

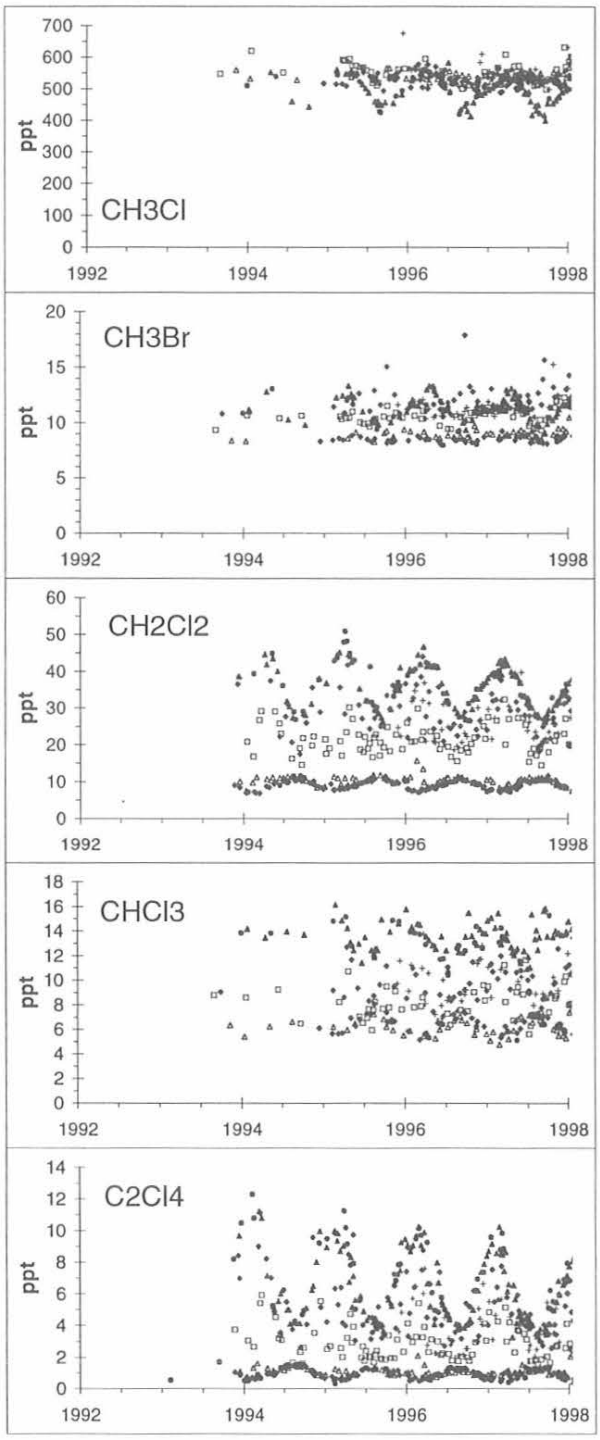

Fig. 5.8. Atmospheric dry mole fractions (ppt) determined for selected chlorinated trace gases and CH_3Br. Symbols are identical to those described in Figure 5.7. Results shown for CH_3Cl, CH_3Br, and $CHCl_3$ are from 2.4-L flasks only. Results plotted for CH_2Cl_2 and C_2Cl_4 are from both 2.4-L and 0.8-L flask samples. All results are based on preliminary calibration scales.

turned off on July 20, 1996, moved and tested, and was operational on July 25th. Because the existing air lines were too short to reach into the new building, a union fitting was put in each line and about 9 m of new Dekabon tubing was added to reach the pump board.

On January 21, 1997, the computer and GC equipment were shut down in the Clean Air Facility at SPO, crated for transport, and quickly moved to the new ARO. By January 27 all of the equipment was operational again. The very long air sampling lines were moved and cable tied above the snow with other lines on poles to avoid being crushed by people and equipment. Since the distance from the ARO to the sampling tower was closer than the Clean Air Facility to the tower, the excess air line was coiled up in the crawl space below the first floor where the equipment is located.

Three 4-channel Chromatograph for Atmospheric Trace Species (CATS) (old STEALTH system) type gas chromatographs are currently in operation at HFM, ITN, and LEF. A fourth single-channel version measures N_2O and SF_6 at ALT. The RITS 3-channel GCs will be phased out after a 6-month comparison with the CATS system. This period will be used to ensure comparable results. The first CATS system was shipped in December 1997 and was installed at SPO in January 1998.

Data Analysis

A thorough review of our current calibration scale for CFC-12 was undertaken before an intercomparison meeting with AGAGE staff in May 1997. This resulted in changes on the order of -2% to assigned mixing ratios for all calibration tanks used at the field sites from 1993 to the present. Likewise, by applying the same techniques to other gases, the calibration scales for CFC-11, nitrous oxide, methyl chloroform, and carbon tetrachloride have changed, though not dramatically. All data presented here have had these corrections applied and are our current best estimates of what is happening in the global tropospheric atmosphere.

The revised, globally averaged maximum CFC-11 mixing ratio was 272.5 ppt in late 1993 (Figure 5.9). The mixing ratio was 268.8 ppt at the end of 1997, the growth rate was -1.3 ppt yr^{-1}, and the interhemispheric difference was 2.6 ppt. The global CFC-12 mixing ratio at the end of 1997 was 531.4 ppt (Figure 5.10). The growth rate slowed until mid-1996 and now appears to be holding steady at 3.6 ppt yr^{-1}. The average interhemispheric difference continues to decline and was 7.9 ppt in late 1997.

Carbon tetrachloride has been decreasing in the troposphere over the last 6 years at the rate of -0.7 ppt yr^{-1}. At the end of 1997 the global mixing ratio was 102.0 ppt and the interhemispheric difference about 1.4 ppt (Figure 5.11). The revised calibration scale has increased mixing ratios by approximately 1% from 1993 and the rate of decrease is less than previously reported.

As noted in section 5.1.2, methyl chloroform mixing ratios continue to decrease in the atmosphere (Figure 5.12). At the end of 1997 the global mixing ratio was 76.9 ppt, and the interhemispheric gradient was near zero. The global distribution in 1997 reflects the distribution of sinks more than sources now that emissions have dropped substantially.

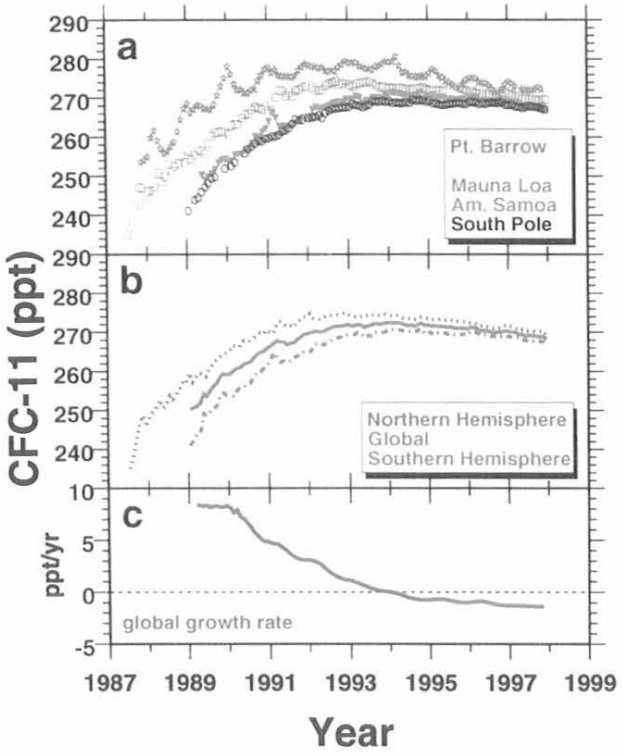

Fig. 5.9. (a) Monthly average CFC-11 mixing ratios in ppt from the in situ GCs, (b) hemispheric and global average mixing ratios, and (c) global average growth rate in ppt yr^{-1}.

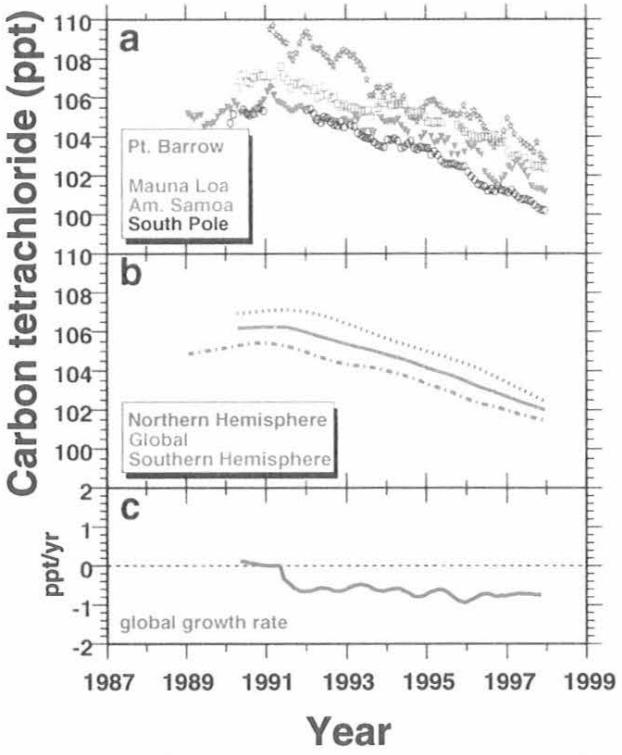

Fig. 5.11. (a) Monthly average carbon tetrachloride mixing ratios in ppt from the in situ GCs, (b) hemispheric and global average mixing ratios smoothed using a LOWESS routine, and (c) global average growth rate in ppt yr^{-1}.

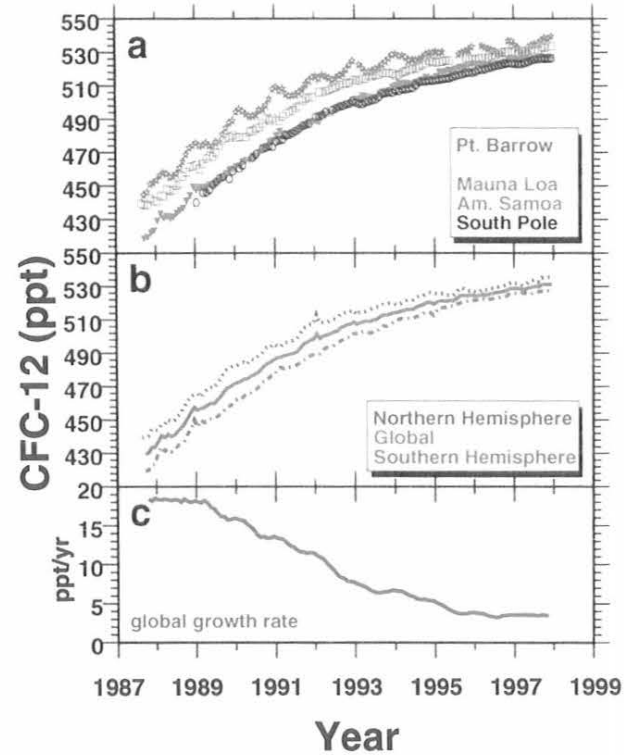

Fig. 5.10. (a) Monthly average CFC-12 mixing ratios in ppt from the in situ GCs, (b) hemispheric and global average mixing ratios, and (c) global average growth rate.

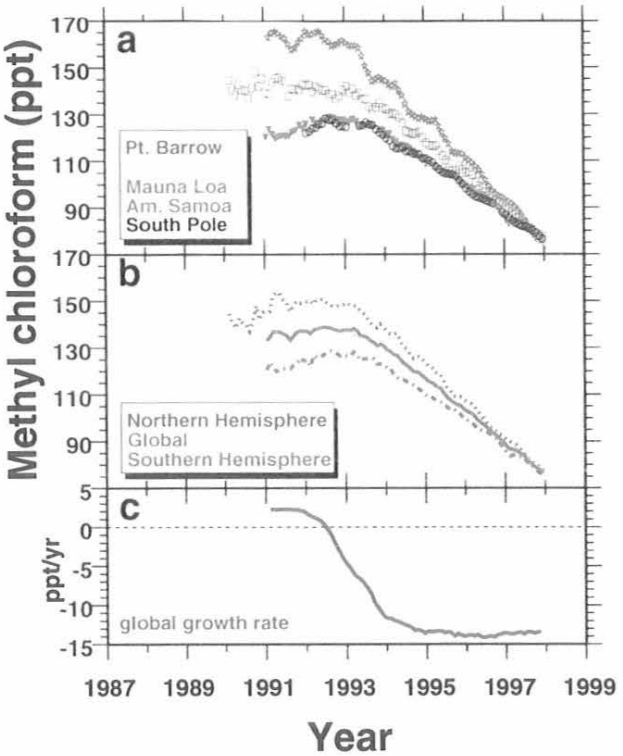

Fig. 5.12. (a) Monthly average methyl chloroform mixing ratios in ppt from the in situ GCs, (b) hemispheric and global average mixing ratios, and (c) global average growth rate.

The atmospheric burden of nitrous oxide continued to increase at an average rate of 0.68 ppb yr^{-1} (RITS measurements) over the past 4 years (Figure 5.13). The global mixing ratio at the end of 1997 was 313.1 ppb and the average hemispheric difference over the 1987-1997 period was 1.2 ppb. There is an annual cycle in the southern hemisphere that is in phase with the annual cycle in the northern hemisphere, generally peaking in the first quarter of each year.

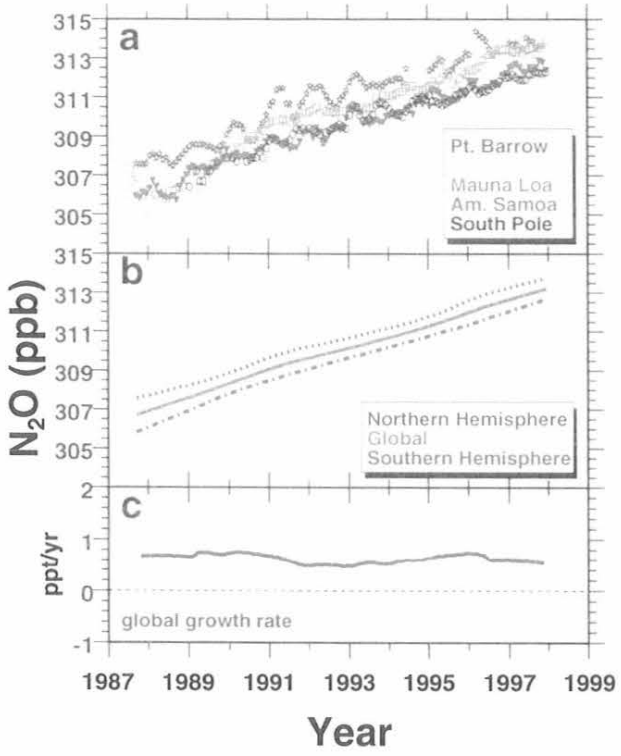

Fig. 5.13. Monthly average nitrous oxide mixing ratios in ppt from the in situ GCs, (b) hemispheric to global average mixing ratios, and (c) global average growth rate.

Chromatography and Software

Each in situ gas chromatograph system is custom designed specifically for each site. Table 5.5 lists the compounds to be sampled by the new in situ gas chromatograph at the CMDL observatories.

Chromatography is controlled and data acquired with custom programs developed on the QNX operating system run on personal computers. QNX is a UNIX-based operating system with structured C programming language support. As a multitasking operating system, QNX provides simultaneous programming functions that allow for concurrent control, data acquisition, user interface operation, and data retrieval. The enhanced capabilities of QNX have allowed the addition of features that take advantage of available technology.

TABLE 5.5. Peak Characteristics on Four-Channel GC at SPO

Compound	Channel	Retention Time (sec)	Peak Window Size (sec)
N_2O*	1	250	40
SF_6*	1	310	20
N_2O†	2	50	30
CFC-12†	2	70	30
CFC-11†	2	215	70
CFC-11‡	3	200	20
CFC-113‡	3	235	20
$CHCl_3$‡	3	350	20
CH_3CCl_3‡	3	425	30
CCl_4‡	3	485	30
TCE‡	3	590	40
PCE‡	3	1230	80
HCFC22§	4	640	30
CH_3Cl§	4	710	40
CH_3Br§	4	1148	60

*Porapak Q column
†Unibeads 1s column (replacing old Porasil a column)
‡OV101 column
§Capillary column (Poraplot Q)

The control functions of the in situ gas chromatograph fall into two categories: those controlled by a custom digital interface and those controlled by an RS-485 network. Sample selection, chromatographic valves, cut-off solenoids, and flow controllers are controlled by a custom digital interface. Temperature controllers use an RS-485 network. Two data acquisition circuit boards handle input from the gas chromatograph electrometers, temperature sensors, and pressure sensors. Chromatographic data from the electrometers and engineering data are stored in a file buffer on the hard drive of the computer. Raw chromatograms and a representative subset of the engineering data are extracted from the buffer, compressed, and stored in a retrieval sub-directory, set up as a first-in-first-out (FIFO) on the hard drive and archived on 100 mb Iomega Zip disks at the site.

A computer workstation at CMDL Boulder automatically retrieves the chromatographic and engineering data from the in situ gas chromatograph on a daily basis for processing. Routines for this retrieval were programmed using TCP/IP - Internet links. Additional programs for use in trouble-shooting and routine maintenance have been included in the QNX software. A World Wide Web (WWW) site allows scientists and technicians to determine the operational status of the instrument system over the Internet. The WWW page includes real-time and near real-time engineering and chromatographic data displayed in tabular and graphic formats. This user interface, accessed with widely available WWW browser software, adds considerable flexibility for scientists and technicians to anticipate problems to resolve quickly.

5.1.4. Gravimetric Standards

The NOAH standards project was expanded in 1996 with the addition of one full-time research assistant. A new gas chromatograph, similar to the CATS GC, was tested and

calibrated. The new GC will provide measurement of CH_3Br, CH_3Cl, and HCFC-22 in the standards laboratory and eliminate the need for three separate GCs for measuring the other seven gases. Thirty gravimetric standards were prepared during 1996-1997. A total of 132 secondary and primary gravimetric standards were analyzed in the standards laboratory. Thirty-three standards were made for outside organizations and other NOAA laboratories. The leader of the standards project left for a new position at NIST at the end of 1997.

One of the major goals of the standards program was to provide a uniform standardization between the major networks responsible for monitoring N_2O and many halocompounds in the atmosphere. A workshop was held during May 1997 in Boulder to begin this process. A series of round-robin tanks are being distributed for intercomparison. A number of tests involving cylinder stability are underway.

Calibrations for CFC-12, methyl chloroform, and carbon tetrachloride were revised since the last report [*Elkins et al.*, 1996b]. All atmospheric CFC-12 data reported after 1993 were about 2.3% higher than actual. The reason for the error was the reliance on a set of 1993 standards that deviated from the rest of the standards which were made in 1991 and 1997 (Figure 5.14). Removal of that set resulted in better agreement (within 1%) for atmospheric measurements of CFC-12 between the CMDL and AGAGE networks. New gravimetric standards were prepared for CH_3CCl_3 and CCl_4 in 1996. After comparing standards for all gases, the same 1993 set was found to have problems with these gases too (Figure 5.15). The values of the 1993 CCl_4 standards are on average 4% lower near ambient levels (102 ppt) than those made in 1991 and 1997. The net effect to atmospheric CCl_4 values (RITS GCs) reported in the last summary report is small, because a calibration tracking error in the opposite direction was found. The 1993 CH_3CCl_3 standards exhibited greater imprecision than the combined 1991 and 1996 sets but no significant offset. The atmospheric values are relatively unchanged from the last summary report. The new scales for CH_3CCl_3 and CCl_4 give atmospheric values that are about 8 ppt and 3 ppt higher in 1997 than those measured by AGAGE. An exchange of weighed pure solvents in sealed microtubes is planned to test methods used by both networks.

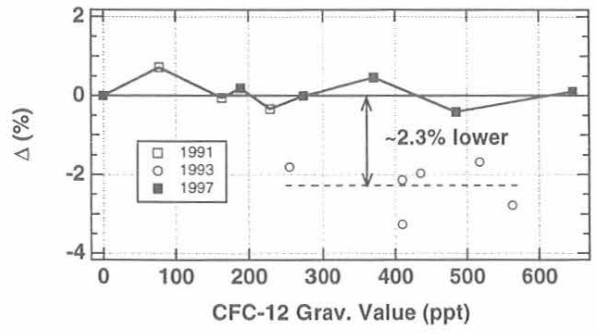

Fig. 5.14. The relative difference in percent (observed-gravimetric value) for CFC-12 standards versus the gravimetric value for those standards made in 1993 and those prepared in 1991 and 1997 for the complete range of ambient ppt mixing ratios.

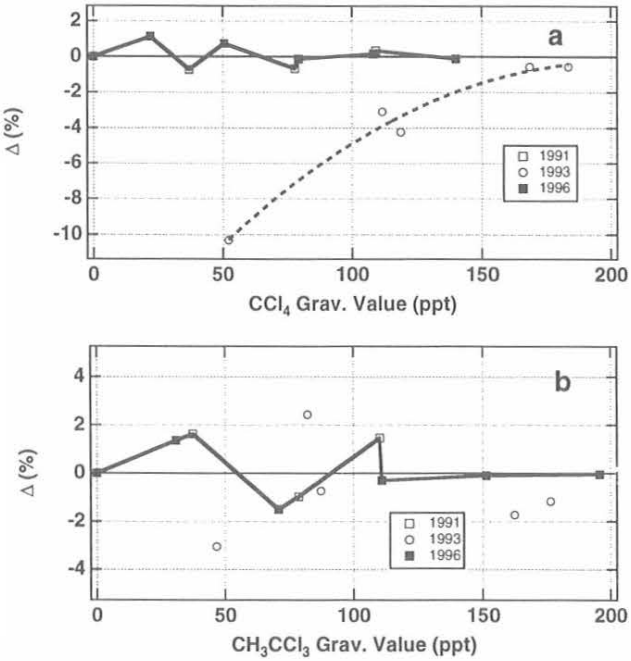

Fig. 5.15. The relative difference (%) in the observed-gravimetric value for (a) CCl_4 and (b) CH_3CCl_3 standards versus the gravimetric value for those standards made in 1993 and those prepared in 1991 and 1997 for the complete range of ambient ppt mixing ratios.

5.2. Stratospheric Measurements

5.2.1. Aircraft Projects-ACATS-IV

ASHOE/MAESA: Stratospheric and Atmospheric Lifetimes of Source Gases

The environmental impact of the measured anthropogenically-produced source gases depends, among other factors, on the rate at which they break down, releasing ozone-depleting chemicals in the stratosphere, i.e., on their stratospheric lifetimes. For many compounds studied here, there exist no significant tropospheric sinks (e.g., N_2O, CCl_4, CFCs 11, 12, and 113), so the stratospheric lifetime, defined here as the atmospheric lifetime with respect to stratospheric loss, is identical to the atmospheric lifetime for these species. A long atmospheric lifetime means a greater ozone depletion potential and a greater global warming potential than similar source gases with shorter lifetimes.

Plumb and Ko [1992] showed that in the "global diffuser" model, stratospheric transport can be described by a simple one-dimensional flux-gradient relationship. If the mixing ratios of two long-lived tracers, σ_1 and σ_2, are in steady state, then the slope of their correlation in the lower stratosphere equals the ratio of their stratospheric removal rates. Thus,

$$\frac{\tau_1}{\tau_2} \equiv \frac{d\sigma_2 B_1}{d\sigma_1 B2} \qquad (1)$$

where B_i is the total atmospheric burden for species i, and τ_i is its steady-state stratospheric lifetime, equal to the steady-state atmospheric lifetime for species without tropospheric sinks. *Volk et al.*, [1997] showed that under the same conditions, steady-state stratospheric lifetimes may be derived from the gradient of the steady-state tracer mixing ratio, σ, with respect to the mean age of stratospheric air [*Hall and Plumb*, 1994], Γ, in the measured air parcels:

$$\frac{B}{\tau} = -\frac{d\sigma}{d\Gamma} M_u \qquad (2)$$

where M_u is the total number of molecules above the tropopause, and the tracer gradient with respect to age, $d\sigma/d\Gamma$, needs to be evaluated at $\Gamma = 0$ which is assumed to be the extratropical tropopause.

If the tropospheric mixing ratio of the tracer is changing with time, part of the tracer gradient at the tropopause is due to accumulation in the troposphere and $1/\tau_i$ in either equation (1) or (2) has to be replaced with $\tau_i^{-1} + B_u'/B$, where τ_i is the instantaneous lifetime and B_u' is the total accumulation rate above the tropopause. *Volk et al.* [1997] proposed an alternative method of accounting for tropospheric growth and non-steady-state mixing ratios, χ, to obtain steady-state lifetimes. In this method, one deduces the correction factors $C(\chi_i)$ for each species using the tracer gradient with respect to age at the tropopause, $d\chi_i/d\Gamma$, the time series of tropospheric mixing ratios of the respective species during a 5-year period prior to the stratospheric observations, and estimates of the width of the stratospheric age spectrum from three-dimensional transport models [*Hall and Plumb*, 1994].

Volk et al. [1997] showed that corrected steady-state correlation slopes defined as:

$$\frac{d\sigma_i}{d\sigma_{CFC-11}} = \left(\text{observed} \frac{d\chi_i}{d\chi_{CFC-11}} \right) \bullet \frac{C_i}{C_{(CFC-11)}} \qquad (3)$$

can be used in equation (1) to derive steady-state lifetimes based on a given CFC-11 reference lifetime. Mixing ratios of N_2O from the Airborne Tunable Laser Absorption Spectrometer (ATLAS) [*Loewenstein et al.*, 1989] and ACATS CFC-113 plotted against ACATS-IV CFC-11 (Figure 5.16a, b) are used to calculate the observed gradient ($d\chi_i/d\chi_{CFC-11}$) in Table 5.6. ATLAS N_2O measurements were calibrated from CMDL N_2O standards and agreed with onboard ACATS N_2O measurements to within ±2%. ATLAS N_2O data are used here to increase the number of measurements used by a factor of 2. The steady-state stratospheric lifetime for a source gas using the reference lifetime for CFC-11 is:

$$\tau = \frac{\left(\tau_{CFC-11} \frac{\bar{\sigma}}{\sigma_{CFC-11}} \right)}{\left(\frac{C_i}{C_{CFC=11} d\chi_{CFC-11}} \Big|_{[CFC-11]=\text{tropopause}} \right)} \qquad (4)$$

where $\bar{\sigma}$ is the mean atmospheric mixing ratio with the

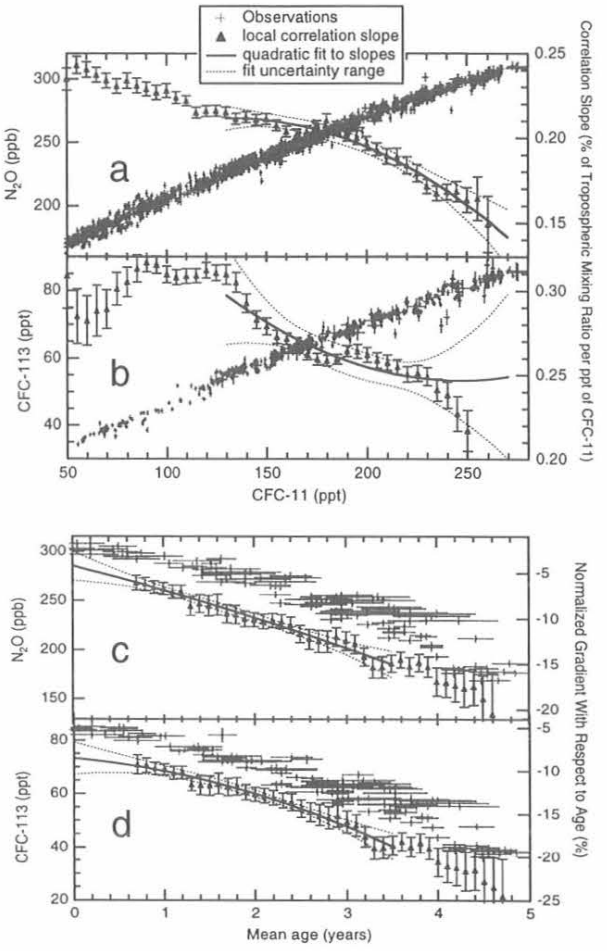

Fig. 5.16. Two methods used to calculate the stratospheric lifetimes from aircraft data. The mixing ratio and its gradient of (a) ATLAS N_2O and (b) ACATS CFC-113 against a lifetime reference molecule such as CFC-1 and the mixing ratio and its gradient of (c) ATLAS N_2O and (d) ACATS CFC-113 against the mean age of the air mass calculated from airborne SF_6 measurements. Observations (pluses, where symbol size indicates uncertainty, left axes), normalized local correlation slopes (triangles with error bars, right axes), and quadratic fits with uncertainty envelopes (lines, right axes) are shown.

gradient calculated at the tropopause. From Figure 5.16 and Table 5.6, the steady-state atmospheric and stratospheric lifetime for N_2O is 122 ± 22 years and for CFC-113 is 100 ± 32 years using a CFC-11 reference lifetime of 45 ± 7 years using equation (4).

The steady-state gradient, $d\sigma_i/d\Gamma$ defined as (observed $d\chi i/d\Gamma$) times $C(\chi i)$, is used in equation (2) to obtain the steady-state lifetime using the "mean age" technique. The steady-state stratospheric lifetime for a source gas based on mean age becomes

$$\tau = -\bar{\sigma} M_a \Big/ \left(M_u C \frac{d\chi}{d\Gamma}\Big|_{\Gamma=0} \right) \qquad (5)$$

TABLE 5.6. Stratospheric Steady-State Lifetimes From *Volk et al.* [1997] Compared to Current Reference Values

Source Gas	Observed $d\chi i/d\Gamma$ (ppt yr^{-1} ± %)	Steady-State Lifetime Based on Age (year)*	Observed $d\chi i/d\chi_{CFC-11}$ (ppt/ppt, ± %)	Steady-State Lifetime Based on CFC-11 (year) $\tau_{CFC-11} = 45 \pm 7$ yr^{-1}*	WMO/IPCC Reference Lifetimes (year)	Correction Factor $C(c_i)$
N_2O	-13,000 ± 38%	124 ± 49	436 ± 11%	122 ± 22	120†	0.97 ± 0.02
CH_4	-109,000±48%	84 ± 35	3230 ± 10%	93 ± 14	120‡	0.96 ± 0.02
CFC-12	-43.8 ± 25%	77 ± 26	1.29 ± 7%	87 ± 17	105†	0.77 ± 0.07
CFC-113	-7.3 ± 22%	89 ± 35	0.212 ± 20%	100 ± 32	85†	0.65 ± 0.12
CFC-11	-33.5 ± 28%	41 ± 12	(1)	(45 ± 7)	50†	0.96 ± 0.02
CCl_4	-15.9 ± 32%	32 ± 11	0.515 ± 3.6%	32 ± 6	42†	1.03 ± 0.02
CH_3CCl_3	-16.3 ± 35%	30 ± 9	0.472 ± 10%	34 ± 8	45‡	1.14 ± 0.13
H-1211	-0.84 ± 31%	20 ± 9	0.0237 ± 7%	24 ± 6	36§	0.90 ± 0.10

*Uncertainty of CFC-11 lifetime is not included in uncertainty estimate.
†[*WMO*, 1995], Table 13-1.
‡[*IPCC*, 1995b], Table 2.2.
§[*WMO*, 1992], Table 6.2, scaled to τ_{CFC-11}= 45 years.

where M_a is the total atmospheric mass (5.13×10^{18} kg) and M_u is the total atmospheric mass in the upper atmosphere above the tropospause (1.1×10^{18} kg). From Figure 5.16 the steady-state atmospheric and stratospheric lifetime for N_2O is 124 ± 49 years and for CFC-113 is 89 ± 35 years based on "mean age" calculated using equation (5) (Table 5.6). The uncertainties on the lifetimes using mean age are less precise than those calculated from the reference lifetime method because SF_6 was only measured during the last quarter of the flights during ASHOE/MAESA.

Lifetime results from the two methods presented in *Volk et al.*, [1997] are consistent with each other (see Table 5.6). In most cases the calculated stratospheric lifetimes from observations are shorter than the World Meteorological Organization (WMO) or the Intergovernmental Panel on Climate Change (IPCC) reference lifetimes derived from photochemical models. Since the derived stratospheric lifetimes are identical to the atmospheric lifetimes for many of the source gases in Table 5.6, the shorter lifetimes also would imply a faster-than-predicted recovery of the ozone layer following the complete phase out of industrial halocarbons.

STRAT Campaign

The primary goal of the Stratospheric Tracers of Atmospheric Transport (STRAT) mission was to measure the morphology and dynamic properties of long-lived tracers as functions of altitude, latitude, and season to help determine the rates for global-scale transport and future stratospheric distributions of high-speed civil transport (HSCT) exhaust. ACATS-IV participated in four out of six STRAT deployments and was flown on a total of 31 flights that spanned a range of latitudes (2.1°S to 59.1°N), predominantly at 15 to 21 km altitudes (potential temperature, θ = 360 to 510 K). These flights included four southbound survey flights into the tropics from Barbers Point, Hawaii (22°N), four northbound survey flights to nearly 60°N from Moffett Field, California (38°N), and 23 midlatitude flights from both locations.

Sulfur hexafluoride has no known sinks below the stratopause (τ = 3200 years, [*Ravishankara et al.*, 1993] and has exhibited a steady rate of growth of 6.7% yr^{-1} in recent years [*Geller et al.*, 1997]. It is used to study atmospheric transport processes and the age of air masses in the upper atmosphere [*Geller et al.*, 1997; *Volk et al.*, 1997; *Wamsley et al.*, 1998]. The age of air masses at the tropical tropopause is defined as zero. Tropospheric air masses that have not yet reached the tropopause are associated with negative ages. ACATS-IV measurements of SF_6 in the northern midlatitude upper troposphere during November 1995 and December 1996 show that mixing ratios increased by approximately 0.28 ppt in 13 months, which is close to the 0.26 ppt expected from the documented growth rate (Figure 5.17). Figure 5.18 shows the convergence of the November 1995 and December 1996 data sets above θ = 450 K that are due to the increased effects of stratospheric mixing with age of the air.

In the tropics (2°S to 20°N) vertical profiles of the mixing ratios of trace gases with different lifetimes conform to the results of *Volk et al.* [1996] (that is, entrainment into a "leaky tropical pipe"). This entrainment of midlatitude air results in "proportionally mixed" tropical profiles, which for CFC-11 are shifted about 15% from the unmixed tropical model line of *Volk et al.*, [1996] shown in Figure 5.18. In the altitude range important for HSCT (16-20 km), ACATS-IV tropical data show several intrusions of midlatitude air into the tropics, denoted by several measurements that lie far to the left of the proportionally mixed tropical profiles (θ = 410-450 K and at 480 K, Figure 5.19). The trace gas mixing ratios of the intruding air masses are about 50% lower than the proportionally mixed profiles and are more typical of midlatitude air from much further aloft (θ >440 K; the midlatitude data are shown by a red line and a 95% prediction band on Figure 5.18). Similar, but weaker intrusions of midlatitude air at the same θ can also be seen in other tropical data [*Elkins et al.*, 1996a; *Volk et al.*, 1996].

The entrainment of midlatitude air into the tropics is illustrated further by looking at the age of the air in the tropical region. The age measured during the flight of December 11, 1996, reaches 1.8-2.3 years at both 410-450 and 480 K surfaces in the latitude range from 12°N to

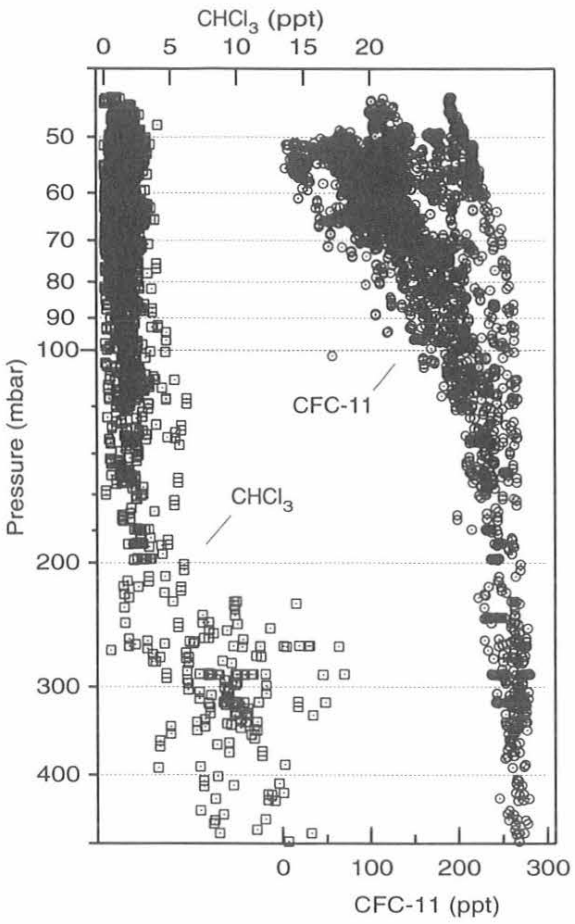

Fig. 5.21. Chloroform and CFC-11 versus pressure. CFC-11 approaches 10 ppt at 26 km and zero at about 30 km in midlatitudes.

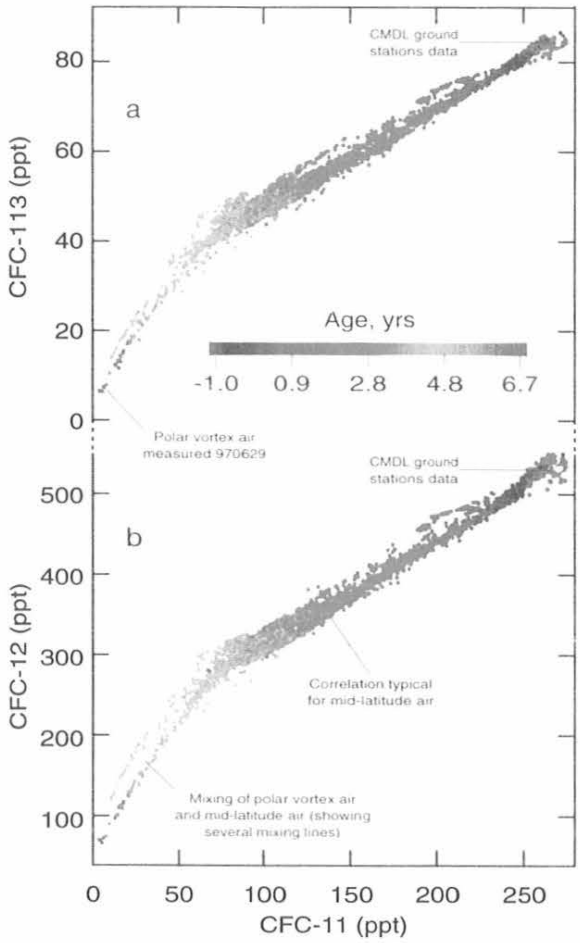

Fig. 5.22. Tracer-tracer correlations, POLARIS mission. (a) Medium-lived CFC-113 (τ = 85 years) shows some separation in the part of the plot depicting mixing; (b) Longer-lived CFC-12 (τ = 102 years.) shows several better separated lines of mixing of air parcels with different age and, subsequently, compounds ratio determined by difference in photolysis rate.

during POLARIS (Figure 5.23), calculated from ACATS-IV SF_6 measurements, demonstrates that the tropical lower stratosphere is characterized by young air (0.3 to 0.8 year average) and that the lines of stable tracer mixing ratios (isopleths) typically follow θ surfaces. Air masses older than 4 to 5 years are generally found poleward of 50°N, but in some cases were observed around 40°N. The oldest air masses encountered during POLARIS were 6.7 years at about 60-65°N in late June 1997.

5.2.2. High Altitude GC Tracer Measurements Project: OMS/STRAT/POLARIS

LACE is a relatively new, three-channel GC instrument (Figure 5.24). It was constructed to extend real time GC measurements of atmospheric tracers such as those measured with the ACATS instrument, to higher altitudes of up to 32 km where, particularly in the tropics, a larger portion of ozone production and loss takes place. The LACE instrument has also made improvements on the spatial and temporal resolution by speeding up the chromatography to obtain a sampling period of 70 seconds. Many of these improvements have now been incorporated into the ACATS instrument. During 1997 LACE obtained high-quality data from four balloon flights onboard the Observations of the Middle Stratosphere (OMS) gondola. As part of the STRAT campaign, LACE flew one midlatitude flight out of New Mexico at 35°N and two tropical flights out of Brazil at 7°S. There was also one polar flight out of Fairbanks at 65°N as part of the POLARIS campaign.

The OMS package is currently configured to make measurements pertinent to stratospheric transport issues. Toward this end, LACE has made in situ measurements from the surface to the middle stratosphere of the long lived tracers H-1211, CFC-11, -113, -12, N_2O, and SF_6

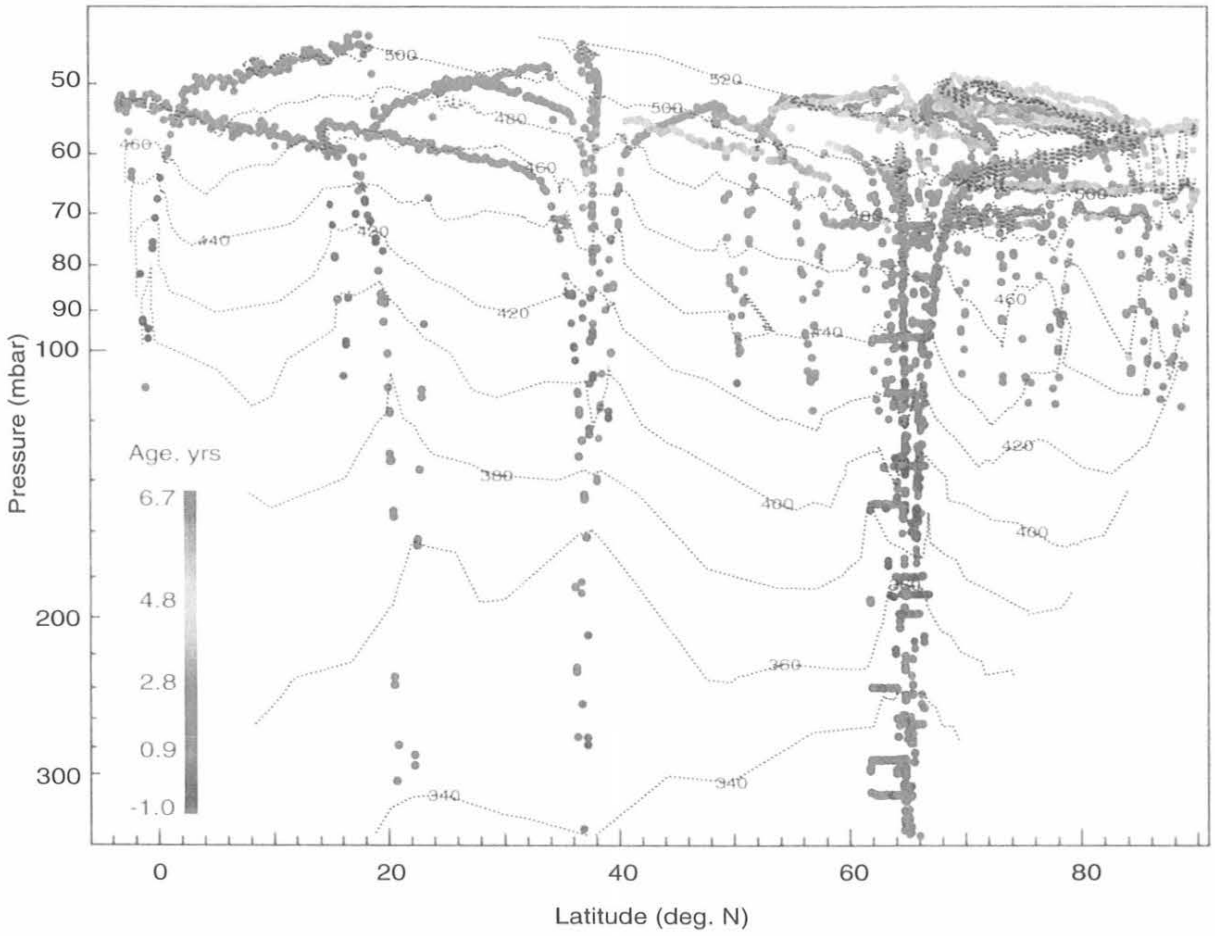

Fig. 5.23. Two-dimensional profiles of altitude and the age of the air based on POLARIS data. The oldest air masses (green) are found at high altitude in the latitude range 60-70°N; younger air is seen at the lower altitudes and latitudes. An age of zero is defined for air at the tropical tropopause, hence negative ages are associated with tropospheric data. Dotted lines show potential temperature surfaces which typically define isopleths (equal mixing ratios).

with a typical precision of between 1% and 4%. The stratospheric lifetimes of these halocarbons and nitrous oxide are dominated by simple photolysis. Their global atmospheric lifetimes span several orders of magnitude. The local photolytic lifetimes of some gases are reduced by 4 orders of magnitude from the tropopause to 32 km. This range in lifetimes covers the dynamic time scales of stratospheric transport. Gas mixing ratios are extremely sensitive to this transport with a strong dependency on vertical flow. Sulfur hexafluoride, however, does not have this altitude-dependent photo-disassociation and has a global atmospheric lifetime greater than 3200 years. Spatial and temporal gradients in the mixing ratio of SF_6 are, therefore, driven by surface emissions which are predominantly in the northern hemisphere. This leads to a large interhemispheric surface gradient and, in this instance, a nearly linear surface growth rate [*Geller et al.*, 1997]. Because there is no known stratospheric sink for SF_6, its sensitivity to transport is driven entirely by the mean transit time from this growing tropospheric source. Unlike the halocarbons, the measured gradients in the value of SF_6 in the stratosphere have only a passive sensitivity to altitude, yet maintain a strong dependency on the time scales of transport [*Volk et al.*, 1997]. Our current precision of SF_6 in the stratosphere is 2%, which translates to 3.5 months of growth.

Although this 3.5 month resolution is adequate to track stratospheric dynamics by defining a mean age of the air parcel since entering the stratosphere, it is not adequate to track transport within the free troposphere other than interhemispheric exchange. Nonetheless, tropospheric vertical gradients with both temporal and latitudinal dependence appear to persist. The interhemispheric surface gradient is believed to be transported into the free troposphere between 30°N and 30°S in a time scale comparable to or faster than this 3.5-month resolution. A measurement of these vertical gradients in the SF_6 mixing ratio below the 380 K isotherm coupled

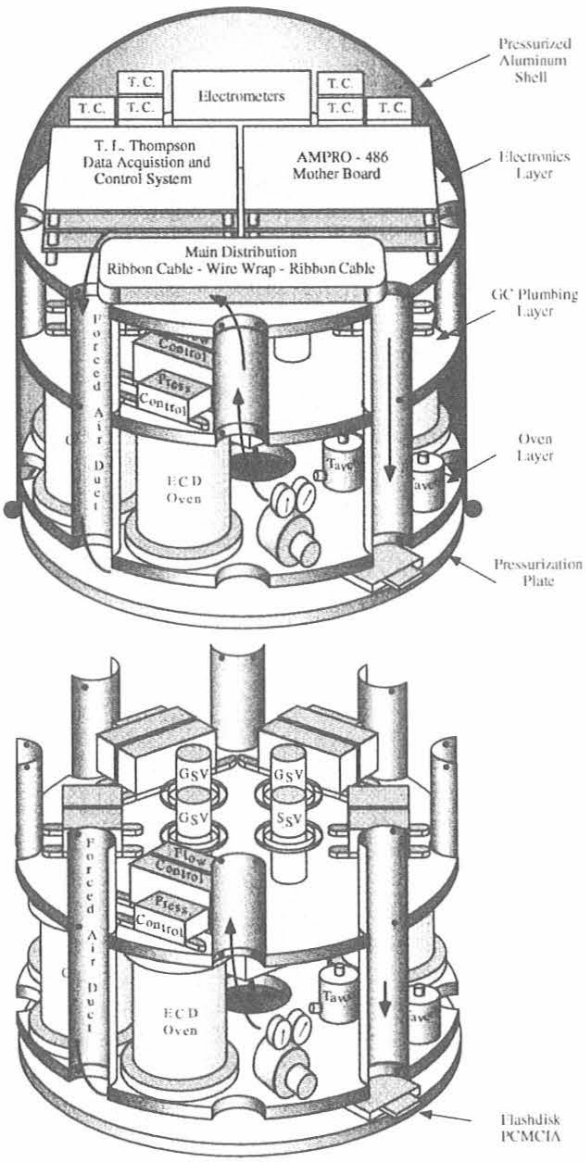

Fig. 5.24. The LACE GC is constructed in three main layers: an oven layer, a GC plumbing layer, and an electronics layer. The GC is pressurized to maintain an even redistribution of heat through convection. This is especially important at the operating altitude of 32 km. Forced air is circulated through the instrument and along the pressurized shell via air ducts to help dissipate 200 watts of heat.

with the existing measured surface gradients, can be used to quantify tropospheric transport and stratosphere-troposphere exchange. This may also be used to improve the connection between the CMDL global mean value of SF_6 and stratospheric age of the air (e.g., Figure 5.23).

Finally the CFCs and H-1211 mixing ratios represent a significant fraction of the total chlorine and bromine entering the stratosphere. As with the ACATS instrument, an estimate of total chlorine and bromine and their organic-inorganic partitioning can be made from LACE measurements.

Stratospheric Dynamics

Major strides in understanding the interactions between pollutants, production to loss of ozone, and climate forcing have been made in the last decade. Today, uncertainties in transport appear to be the limiting parameter in predictive three-dimensional models. The quality of the upcoming assessment on the environmental impact of existing aircraft and the proposed High Speed Civilian Transport (HSCT) fleet is, therefore, limited by our ability to quantify stratospheric transport. In evaluating LACE data, estimates have been made of entrainment of air from midlatitudes into the tropics, the mean age of an air parcel after crossing the tropical tropopause, and mean flow. Breakdown of the arctic vortex and the resulting cross theta "mixing surface" was also observed in the LACE measurements.

As discussed by *Plumb and Ko* [1992], tracer-tracer correlations between simple photochemical species are robust as long as quasi-horizontal mixing dominates over vertical advection, as in the global diffuser model. In the "tropical pipe" model of *Plumb* [1996] the concept of a tight tracer-tracer correlation is also valid in the midlatitudes and, to a large degree, in the tropics on the other side of the tropical barrier. Mixing across this tropical barrier, the so-called leaky pipe, connects these two regions. This mixing is a major mechanism for transport of midlatitude, lower stratospheric air into the middle and upper stratosphere. This midlatitude mixing into the tropics is also a key uncertainty in the HSCT assessment and has been a primary focus of the OMS platform.

A modified *Volk et al.* [1996] analysis, which quantifies the mixing of air from the extratropical stratosphere into the tropical pipe, has been extended to 32 km by using the new LACE CFC and SF_6 profiles. Two approaches have proven fruitful. The first approach relies on mean vertical advection rates (Q). Local chemical losses of the CFCs are dominated by simple photolysis; therefore, assuming no midlatitude influence, isolated tropical profiles can be calculated given the advection rate, photochemical lifetimes (τ), tropospheric growth rates (γ), and mixing ratios (χ) of the CFCs entering the tropical tropopause (Figure 5.25a,b; dotted black line). These isolated tropical profiles can then be evolved a second time to incorporate mixing from midlatitudes along constant potential temperature (θ) surfaces. This is done with the entrainment time (τ_{in}) assumed to be constant. The tracer continuity is governed by equation (6).

$$\frac{\partial \chi}{\partial \theta} Q = P - \frac{\chi}{\tau} - \gamma\chi - \frac{(\chi - \chi_{mid})}{\tau_{in}} \qquad (6)$$

These profiles have also been corrected for weak $O(^1D)$ chemistry and photochemical production (P) (Figure 5.25a,b).

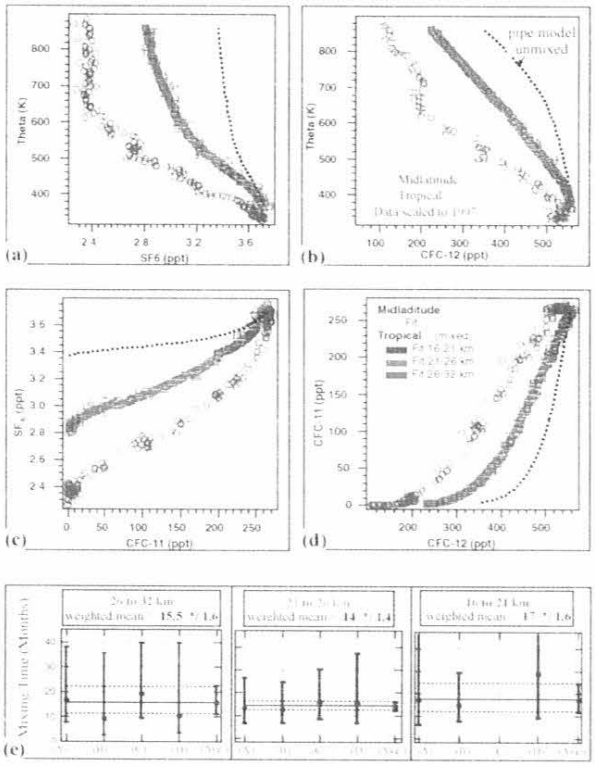

Fig. 5.25. Panels (a) and (b) show least square fits to SF_6 and CFC-12 using equation (6) over three altitude ranges. They are sensitive to uncertainties in vertical advection rates. Panels (c) and (d) show least square fits using equation (2) for CFC-11 versus. SF_6 and CFC-11 versus CFC-12 over the same three altitude ranges. They are, therefore, independent of vertical advection. Panel (e) shows a compilation of entrainment from the four fits in each of the three altitude ranges.

To evaluate whether τ_{in} varies with height, a least squares fit of this second profile to the measured profile is then performed over three altitude ranges. The entrainment time (τ_{in}) is varied as the free fit parameter and is held constant over each given altitude range to stabilize the fits.

One problem that limits this approach is the large uncertainty in the tropical advection rate. Fortunately, the advection rate can be eliminated from the calculation by using tracer-tracer correlation between molecules of differing atmospheric life times. This can be seen by taking the ratio of equation (1) for the mixing ratio Y of one molecule, to equation (1) for the mixing ratio χ of a second molecule.

$$\frac{\partial Y}{\partial X} = \frac{P_y - \left(\tau_y^{-1} + \gamma_y\right)Y - \tau_{in}^{-1}\left(Y - Y_{mid}\right)}{P_x - \left(\tau_x^{-1} + \gamma_x\right)Y - \tau_{in}^{-1}\left(X - X_{mid}\right)} \qquad (7)$$

Because this advection rate Q is common for all molecules in the same air mass moving up the tropical pipe, it drops out of equation (7) (Figure 5.25c,d).

LACE data are consistent with a constant entrainment time of $1.5^{1.9}_{1.2}$ months over the entire range up to 32 km (Figure 5.25e). By 32 km, 90% of the air in the tropical upwelling region is of midlatitude origin because of the total integrated entrainment. A comparison of the first approach (equation 6), which is sensitive to Q, with the second approach (equation 7), which is independent of Q, may help to constrain mean flow in the tropics. This work is consistent with the *Volk et al,* [1996] earlier analysis and is expected to generate a more complete picture of midlatitude intrusions into the tropics when finalized.

Data taken recently in the tropics also revealed air masses that were of midlatitude origin showing the characteristic signature of lower mixing ratios. Surprisingly, the ozone profile did not show the same midlatitude signature and remained representative of tropical air. The chemical equilibrium time for ozone at these locations is fast (weeks to a month), apparently much faster than the mixing time over the spatial scale of these midlatitude intrusions during this time of weak upwelling. These data and the chemical equilibrium time of ozone can, therefore, set lower limits on mixing within the tropical upwelling region.

Sulfur hexafloride has proven to be useful for evaluating transport in the lower and middle stratosphere. Measurements of stratospheric SF_6 permit an accurate determination of the mean age of an air parcel after it crosses the tropical tropopause. Mean age estimates are shown in Figure 5.26 for all LACE flights and three-dimensional model estimates. In general, these models underestimate the age of air as defined by SF_6 distributions. Although increased mixing from mid-latitudes could account for the older measured age in the tropics, the excessively young midlatitude model estimates imply that mean flow in these models is too high.

One important lesson from our OMS balloon launch from POLARIS in Fairbanks was the observation of unmixed and mixed remnants of the polar vortex from the earlier March 1997 arctic ozone depression. Because the remnants of this vortex lasted as late as July, these measurements show one reason why we should continue to sample the arctic. As shown in Figure 5.27, this mixed air is clearly not representative of a typical midlatitude distribution and must continually be monitored to quantify both the chemistry and dynamics that are taking place at the pole.

Atmospheric Dynamics Below the 380 K Isentropic Surface

LACE has taken highly precise measurements of several trace gases in the lowermost stratosphere and upper troposphere, regions for which very little tracer data exist. Measurements of SF_6 and CFC-11, in particular, reveal many interesting features in these regions and their vertical gradients offer constraints on transport time scales. Simulation of these tracer gradients by models is important for an accurate assessment of tracer transport in the lower stratosphere and troposphere where the impact of aircraft exhaust and the transport of greenhouse gases play a key role.

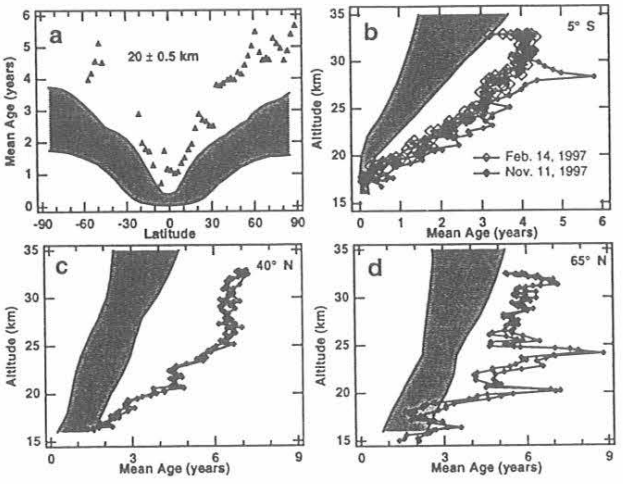

Fig. 5.26. Profiles of mean age of the air from zonally-averaged models (supplied by D. Waugh [private communication, 1998]). This modeled age is plotted with (a) ACATS measured age (triangles) against latitude, and LACE measured age (diamonds) against altitude for (b) the tropics at -5° latitude, (c) the midlatitudes at 35° latitude, and (d) the polar regions at 65° latitude. The shaded region indicates the dominant range of model results. Mean age is taken to be zero at the equator at 20.0 ± 0.5 km.

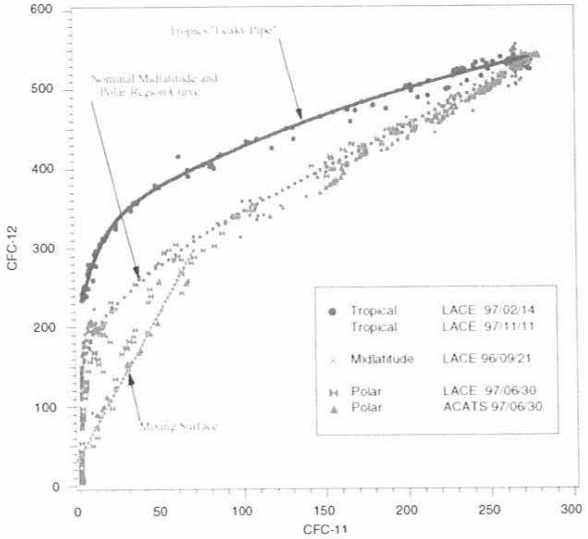

Fig. 5.27. Tracer-tracer correlation plot of CFC-12 versus CFC-11 from LACE on the OMS gondola for flights on September 21, 1996 (midlatitudes), February 14, 1997, and November 11, 1998 (tropics), and June 30, 1997 (POLARIS, polar regions). LACE data are compared against the ACATS data from the POLARIS flight of the ER-2 aircraft on June 30, 1997. The blue line indicates tropical data isolated from the mid and high latitudes by the "leaky pipe," dashed red lines represent a nominal midlatitude and/or polar profile, and the dashed gray line indicates conservative mixing across isopleths due to the anomalously late break down of the polar vortex. This mixing line can only be observed in a tracer-tracer plot over regions that have curvature in the nominal midlatitude profile.

The lowermost stratosphere is that part of the stratosphere that lies between the tropopause and the 380 K potential temperature surface. The lowermost stratosphere is a unique part of the stratosphere, since air can be exchanged isentropically between the stratosphere and troposphere. Thus the lowermost stratosphere contains a mixture of older stratospheric air that has been advected downward by the mean meridional circulation and tropospheric air that has been transported isentropically. The relative importance of downward advection and isentropic transport largely depends on season and location.

Figure 5.28 shows profiles of SF_6 and CFC-11 from the Ft. Sumner flight on September 21, 1996. The 380 K and tropopause heights are indicated on the figure and lines are drawn through the data in each height region. The two profiles have different vertical gradients in the lowermost stratosphere. CFC-11 has almost no vertical gradient below the 380 K surface, while SF_6 has a large vertical gradient in the lowermost stratosphere and a small but still noticeable gradient in the upper troposphere. The constant CFC-11 mixing ratio suggests that the gradients seen in the SF_6 profiles are of tropospheric origin. Downward advection would have a larger effect on CFC-11 because of its more rapid decrease above the 380 K surface. Weak downward flow across the 380 K surface at the time of our flight is consistent with the seasonality of the mean meridional circulation in the stratosphere and the midlatitude location.

The vertical gradient in SF_6 from the Ft. Sumner flight is, therefore, assumed to be due to an interplay between

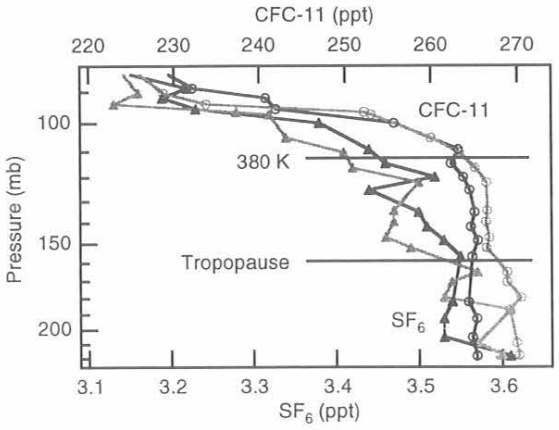

Fig. 5.28. Profiles of SF_6 and CFC-11 from the September 21, 1996, Ft. Sumner, New Mexico, flight. The tropopause and 380 K surfaces are indicated on each plot and rough linear fits to the data are included in each region.

isentropic mixing from the tropical upper troposphere and residence time of air in the lowermost stratosphere. Were it the result of growth, the vertical gradient in SF_6 would

represent a 9-month age difference over the depth of the lowermost stratosphere. The time scale of isentropic mixing between the tropopause and the northern midlatitudes is on the order of a month or less and the flushing time of the northern hemisphere lowermost stratosphere is thought to be roughly 4 or 5 months. Therefore, some of the vertical gradient in the lowermost stratosphere could be caused by transport of the interhemispheric gradient of surface SF_6 to the upper troposphere. Some portion of the interhemispheric gradient in SF_6 is likely to be mapped along the tropopause from the tropics to the midlatitudes. As tropospheric air is isentropically mixed into the midlatitude lowermost stratosphere, the latitudinal tropopause gradient will contribute to the vertical gradient of SF_6 in the lowermost stratosphere.

This gradient in SF_6 along the tropopause may have a strong dependence upon seasonal variability of tropospheric transport, coupled with the interhemispheric gradient of SF_6 at the surface. Profiles of SF_6, which have been normalized to remove the growth rate for the two Brazil flights, are shown in Figure 5.29. The February Brazil flight has SF_6 mixing ratios in the upper troposphere that are close to the global mean surface value and decrease toward the southern hemisphere surface average with decreasing height (Figure 5.29). This profile is consistent with a significant amount of northern hemispheric surface air entering the tropical upper troposphere during February. The monthly mean position of the Hadley circulation was estimated by *Oort and Yienger* [1996]. In January and February the northern hemisphere Hadley cell is shifted south and is also consistent with a significant amount of northern hemispheric surface air being transported into the tropical upper troposphere as suggested by our data.

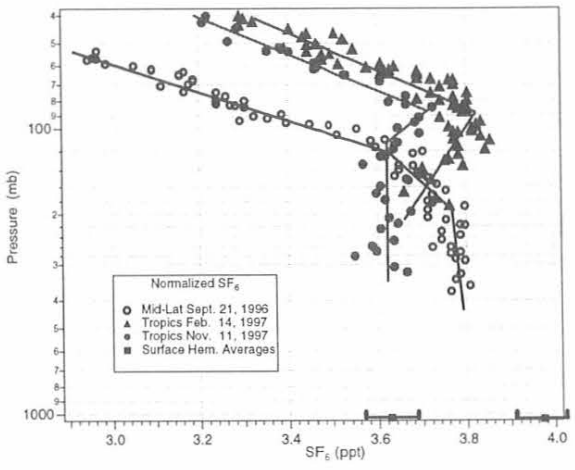

Fig. 5.29. Profiles of SF_6 from the two Brazil flights and the Ft. Sumner, New Mexico, flight normalized to remove the growth rate. Normalized northern and southern hemispheric mean surface mixing ratios from the CMDL network are also included at the bottom of the graph.

The November flight has a nearly constant mixing ratio in the upper troposphere that is close to the southern hemisphere surface average. In October and November the northern hemisphere Hadley cell is weak and shifted north of the equator so the tropical upper troposphere should be dominated by southern hemispheric air at a 7°S, again consistent with our data.

These tropical profiles suggest that the seasonal cycle of the Hadley circulation causes a seasonal cycle in the SF_6 mixing ratios in the tropical upper troposphere. This seasonal cycle will likely cause a seasonal cycle in the latitudinal gradient of SF_6 mixing ratios along the tropopause, since the mean Hadley circulation flow in the upper troposphere is poleward. For the northern hemispheric tropopause we would expect a large gradient during summer, when more southern hemispheric surface air is transported into the tropical upper troposphere, and a weak gradient during winter when mostly northern hemispheric surface air is transported into the tropical upper troposphere. Our midlatitude flight was in September at the beginning of fall when a remnant of the tropopause gradient caused by the summer tropospheric transport could have been present. This also suggests that a small seasonal correction to the connection between stratospheric age of air and the CMDL global average may be needed.

The effects of significant mean downward motion across the 380 K surface on trace gas profiles in the lowermost stratosphere can be seen in Figure 5.30. CFC-12, -11, H-1211, and SF_6 measurements from the June 30, 1997, flight over Fairbanks are shown in this figure along with the heights of the 380 K and tropopause surfaces. Mixing ratios of all four tracers decrease above the tropopause.

This decrease and the vertical gradient in the lowermost stratosphere are largest in the shortest lived tracer, H-1211, which is consistent with the expected effect of downward advection. Subsequently smaller decreases above the tropopause and vertical gradients in the lowermost stratosphere are seen in CFC-11 and CFC-12 which have longer photochemical lifetimes. SF_6 also has a large decrease above the tropopause due not to photolysis but to its growth rate. Air advected down across the 380 K surface in the high latitudes is 2 years older on average, than northern tropospheric air. Therefore the sharp decrease in SF_6 above the tropopause is a result of the growth of SF_6 in the northern high-latitude troposphere during the time air was transported to the high-latitude lowermost stratosphere.

Even though June is a time of relatively weak mean downward flow in the northern hemisphere high latitudes, the tracer data suggest that this flow is the dominant transport into this part of the lowermost stratosphere. It is interesting to note the relative compactness of the profiles above and below the 380 K surface. The lowermost stratosphere appears to be relatively well mixed compared with the stratosphere above the 380 K surface.

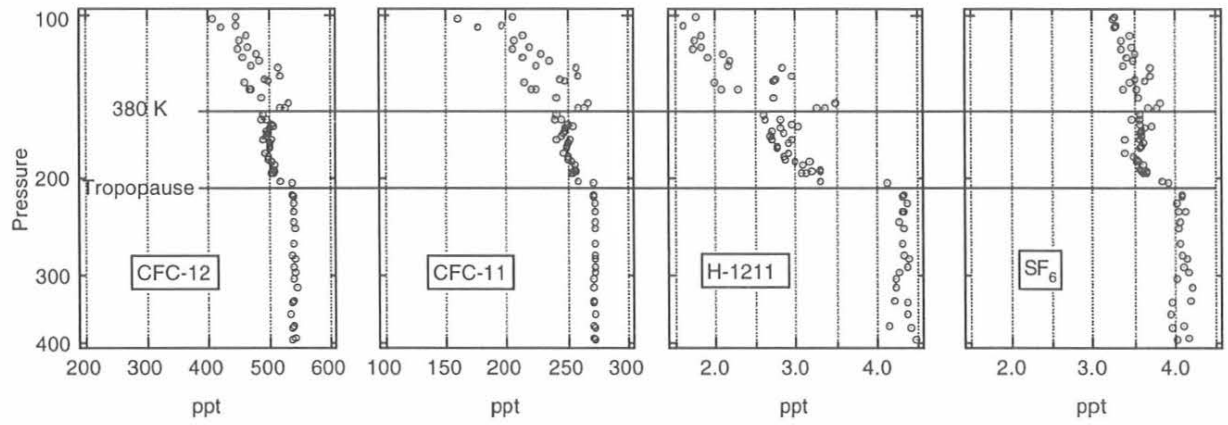

Fig. 5.30. Profiles of CFC-12, CFC-11, H-1211, and SF_6 from the Fairbanks, Alaska, flight. The tropopause and 380 K surfaces are indicated. The three distinct regions, the middle stratosphere (above 380 K), the lowermost stratosphere, and the troposphere, are clearly defined by both the gradients and spread in the data. Relationships between the time scales of mean flow and mixing can be inferred.

5.3. Ocean Projects

5.3.1. Southern Ocean Expedition - BLAST III

The flux of CH_3Br from the world's oceans has been a source of considerable controversy over recent years. Although earlier studies suggested the ocean was a large, net source of atmospheric CH_3Br [*Singh et al.*, 1983; *Singh and Kanakidou*, 1993; *Khalil et al.*, 1993], recent widespread examinations by CMDL of the saturation of CH_3Br in the east Pacific and Atlantic Oceans showed that most of the ocean was undersaturated in this gas [*Lobert et al.*, 1995, 1996; *Butler et al.*, 1995]. Extrapolation of these data indicated that the global oceans were a net sink for atmospheric CH_3Br.

Two subsequently published numerical models, however, suggested that polar and sub-polar oceans might be a large, net source of atmospheric CH_3Br [*Pilinis et al.*, 1996; *Anbar et al.*, 1996]. The two models used production rates based on data published by *Lobert et al.* [1995], presuming them to be either constant over the entire oceanic regions or a function of chlorophyll-a concentration. With chemical degradation being very slow in cold, polar waters, and a very high biological productivity during the austral summer, the predicted saturation anomalies were positive and ranged up to 500%, indicating this polar source could globally outweigh the sinks estimated by *Lobert et al.* [1995]. To resolve this question, CMDL conducted a study to measure the saturation of CH_3Br in the Southern Ocean during a time of high biological productivity (Bromine Latitudinal Air-Sea Transect (BLAST) III, Figure 5.31, *Lobert et al.* [1997]).

The shipboard GC/MS and sampling system was virtually identical to that used during the two previous cruises. On this cruise CH_3Br was also measured with a custom-built GC equipped with an ECD and different columns. Mole fractions from MS and ECD systems agreed, on average, within 0.2 ppt (Figure 5.32, Table 5.7). Measured, dry mole fractions of CH_3Br in the atmosphere were consistent with data from the BLAST I and BLAST II cruises. Most important, however, is that the ocean in this region was consistently undersaturated in CH_3Br with a mean saturation anomaly corrected for physical effects of $-33 \pm 8\%$ (Figure 5.32c, Table 5.7).

Maintaining a steady-state, ~35% undersaturation of CH_3Br in the surface waters in the presence of air-sea exchange requires a minimum in situ degradation rate of about 5.8% d^{-1}, which is a factor of 10 larger than that for chemical degradation alone. The most likely explanation of these findings is that dissolved CH_3Br is being degraded by an additional mechanism other than reaction with H_2O

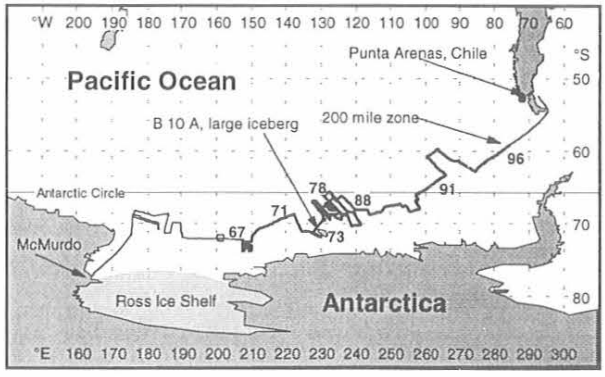

Fig. 5.31. BLAST III cruise track from McMurdo, Antarctica, to Punta Arenas, Chile, aboard the *R/V Nathaniel Palmer*, Cruise 96-02. Numbers along the cruise track indicate the Julian day of year 1996.

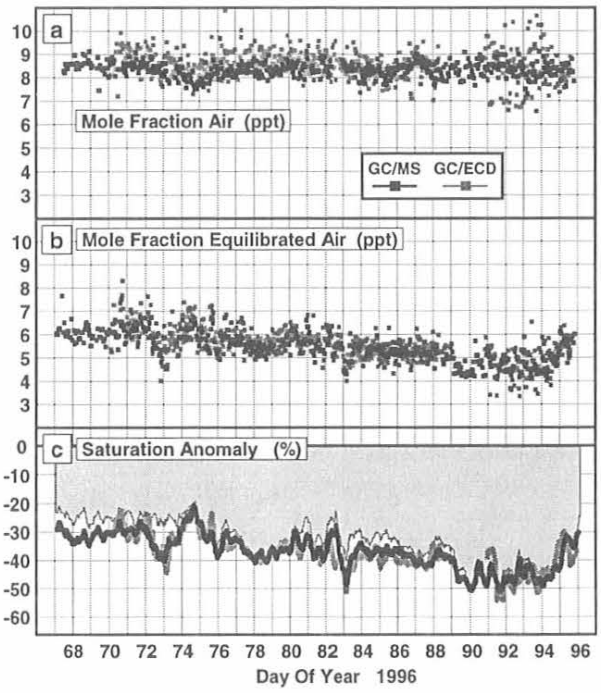

Fig. 5.32. Measurements of methyl bromide in air (a), air equilibrated with surface water (b), and the resulting saturation anomaly (c) for both the GC/MS and the GC/ECD systems. The shaded area in panel (c) represents the saturation anomaly corrected for physical effects calculated from the GC/MS saturation anomaly (black line).

TABLE 5.7. Mean Mixing Ratios of CH_3Br in Air and Equilibrated Water during BLAST III

	GC/MS (ppt)	GC/ECD (ppt)	Mean Saturation Anomaly*	Corrected Saturation Anomaly†
Air	8.3 ± 0.3	8.5 ± 0.7		
Equilibrated water	5.5 ± 0.6	5.6 ± 0.8	-36 ± 7%	-33 ± 8%

*Saturation anomaly = percent departure from equilibrium, calculated from GC/MS data.

†Corrected saturation anomaly = mean anomaly, corrected for physical effects such as those associated with mixing and warming of surface waters [e.g., *Butler et al.*, 1991].

and Cl^-. A significant biological sink for CH_3Br in subtropical waters has been identified recently [*King and Saltzman*, 1997], suggesting that the additional sink might be biological.

Several conclusions can be drawn from this study. First, the Southern Ocean, and probably most high-latitude waters, are a net sink for atmospheric CH_3Br. Second, biological processes, or some chemical processes other than reaction with H_2O or Cl^-, rapidly remove CH_3Br from surface waters. Third, CH_3Br production is neither constant over the global ocean nor strictly dependent upon chlorophyll concentration. The data from this expedition and those from BLAST I and BLAST II suggest that the global ocean is a net sink of 21 (11-31) Gg yr^{-1} for CH_3Br.

5.3.2. Oceanic Uptake of Atmospheric Trace Gases

The atmospheric lifetime of a trace gas is derived from the sum of its sinks or loss rates. Loss to the ocean is a significant sink for some gases. Over the past few years a gridded, finite-increment model was developed to determine the uptake rate constant and partial atmospheric lifetime with respect to oceanic degradation for any trace gas that reacts in seawater. The model, originally developed to study the oceanic uptake of atmospheric methyl bromide (CH_3Br) [*Butler*, 1994; *Yvon and Butler*, 1996; *Yvon-Lewis and Butler*, 1997], is used here to calculate the oceanic uptake rate and partial atmospheric lifetime of chlorocarbons, HCFCs, and HFCs (Figure 5.33, Table 5.8). The oceanic uptake rate (mol yr^{-1}) is defined in the following equation:

$$\text{Uptake} = \frac{K_W A}{H}\frac{r}{n_{tr}}\left(\frac{k_d + K_{biol} + \sqrt{D_z k_z}}{k_d + k_{biol} + \sqrt{\frac{Dk_z}{z} + \left(\frac{K_W}{z}\right)}}\right) \quad (8)$$

The rate constant (k_{ocn}) and lifetime (τ_{ocn}) for this removal process can then be calculated from the following equation:

$$k_{ocn} = \frac{1}{\tau_{ocn}} = \frac{K_W A}{H}\frac{r}{n_{tr}}\left(\frac{k_d + K_{biol} + \sqrt{D_z k_z}}{k_d + k_{biol} + \sqrt{\frac{Dk_z}{z} + \left(\frac{K_W}{z}\right)}}\right) \quad (9)$$

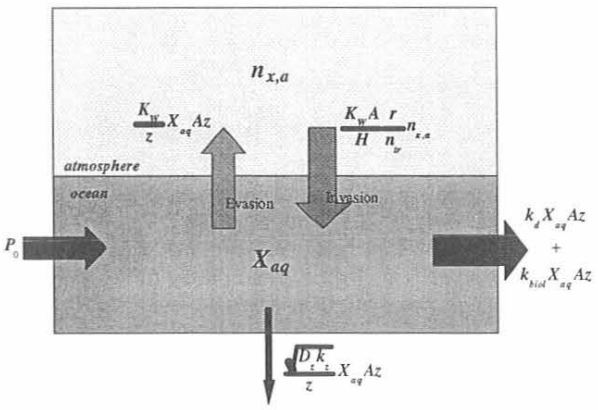

Fig. 5.33. Schematic of the air-sea flux of a trace gas. Terms are as described in Table 5.8.

Initially this equation was applied to a 2° × 2° grid of physical properties in and over the global ocean for the calculation of the partial atmospheric lifetime with respect to oceanic uptake for CH_3Br (Figure 5.34). The inclusion of both the chemical and biological degradation rates for CH_3Br in the ocean resulted in a partial atmospheric lifetime of 1.8 (1.1-3.9) years, which is substantially shorter and more certain than the 3.7 (1.4-14) year estimate calculated by *Butler* [1994], owing to the inclusion of spatial variability in oceanic physical properties and biological degradation rates. The corresponding atmospheric lifetime, including soil to atmospheric sinks for CH_3Br, is 0.7 (0.5-1.2) years.

Oceanic uptake does not appear to be a significant sink for many of the HCFCs and the HFCs (Table 5.9). Because biological degradation processes have not been investigated for most of these trace gases, the term (k_{biol}) was null in these calculations. Model results for these gases depend upon chemical degradation rates alone. The presence of any biological degradation would result in substantially reduced lifetimes. Evidence for the presence of degradation mechanisms other than the hydrolysis reaction used in this model has been observed in the saturation anomaly data for CH_3Br, CH_3Cl, and CCl_4.

The τ_{ocn} values calculated by *Wine and Chameides* [1989] are shorter than those determined by this model because the investigators neglected stratification below the mixed layer [*e.g., Butler et al.,* 1991]. At this time there are no available data on the degradation rate constants

TABLE 5.8. Definition of Terms Used in Oceanic Lifetimes Computation (Equations 2 and 9)

Parameter or Variable	Symbol or formula	Units	References for Calculations
Partial pressure of X	P_X	atm	
Oceanic concentration of X	X_{aq}	mol m^{-3}	
Gas transfer velocity	K_W	m yr^{-1}	1, 2, 3, 4
Solubility	H	m^3 atm mol^{-1}	5, 6, 7, 8, 9
Atmospheric burden of X	$n_{x,a}$	mol	
Surface area of ocean	A	m^2	
Mixed layer depth	z	m	10
Mass of the troposphere	n_{tr}	mol	
Fraction of X in troposphere	r	Unitless	11, 12, 13
Production rate of X	P_0	mol m^{-3} yr^{-1}	
Mixed layer chemical degradation rate constant	k_d	yr^{-1}	8, 14, 15, 16, 17,18, 19
Mixed layer biological degradation rate constant	k_{biol}	yr^{-1}	14,20
Thermocline diffusion coefficient	D_z	m^2 yr^{-1}	10
Thermocline chemical degradation rate constant	k_z	yr^{-1}	8, 14, 15, 16, 17,18, 19
Grid cell index	i	--	
Interhemispheric ratio multiplier (NH and SH)	R_{IHR}	Unitless	20, 21

[1]*Wanninkhof* [1992], [2]*Liss and Merlivat* [1986], [3]*DeBruyn and Saltzman* [1997a], [4]*Wilke and Chang* [1955], [5]*DeBruyn and Saltzman* [1997b], [6]*Moore et al.* [1995], [7]*Gosset* [1987], [8]McLinden [1989], [9]*Johnson and Harrison* [1986], [10]*Li et al.* [1984], [11]*Lal et al.* [1994], [12]*Fabian et al.* [1996], [13]*Chen et al.* [1994], [14]*King and Saltzman* [1997], [15]*Moelwyn-Hughes* [1938], [16]*Gerkins and Franklin* [1989], [17]*Jeffers et al.* [1989], [18]*Wine and Chameides* [1989], [19]*Elliott et al.* [1989], [20]*Lobert et al.* [1995], [21]*Montzka et al.* [1996]

TABLE 5.9. τ_{ocn} and τ for Selected Halocarbons

	τ_{ocn} (y)			τ (y)	
Trace Gas	This Study	Previous	Reference	WMO (1994)*	This Study
CH_3Cl	70(70-79)			1.5	1.46
CH_3CCl_3	94(94-123)	59-128[1]	1	4.8 [4]	4.8
CCl_4	2250			42	42
HCFC-22	2320	110[2]	2	13.3	13.3
HFC-125	10600	>1500[2]	2	36	36
HFC-134a	9100	>1100[2]	2	14	14
HFC-152a	5530	>460[2]	2	1.5	1.5
HCFC-124	1840	360[2]	2	5.9	5.9
HCFC-142b	2060	270[2]	2	19.5	19.5
HCFC-123	635	180[2]	2	1.4	1.4
HCFC-141b	2230	77-360[2]	2	9.4	9.4
$CHCl_3$	715			0.55	0.55
C_2Cl_4	2130000			0.4[5]*	
OCS	13.2	18[3]	3	4.3[6]*	3.2

*C_2Cl_4 OCS lifetimes are from the indicated manuscripts rather than *WMO* [1994]. The only value in this column that included oceanic uptake is that for CH_3CCl_3.

[1]*Butler et al.* [1991], [2]*Wine and Chameides* [1989], [3]*Ulshöfer and Andreae* [1997], [4]*Prinn et al.* [1995], [5]*Wang et al.* [1995], [6]*Chin and Davis* [1995].

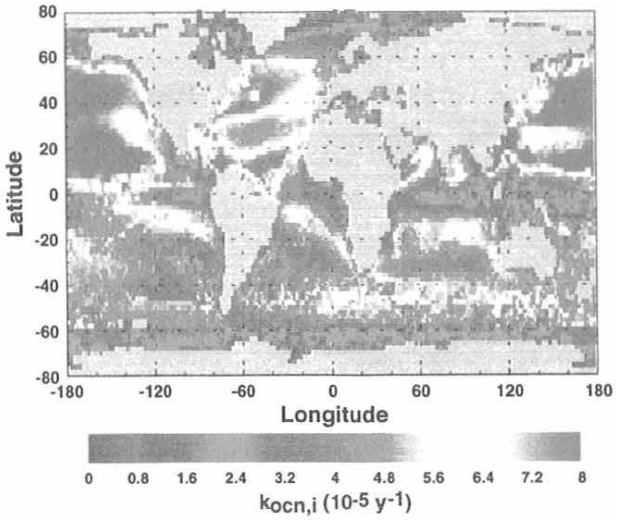

Fig. 5.34. Global distribution of the oceanic uptake rate constant, $k_{ocn,i}$, where $k_{ocn,i} = (1/\tau_{ocn})_i$ for combined chemical and biological aquatic removal of atmospheric CH_3Br. Including biological processes lowers the partial atmospheric lifetime with respect to oceanic loss from 2.7 years [*Yvon and Butler*, 1996] to 1.9 years [*Yvon-Lewis and Butler*, 1997].

and/or solubilities for many of the halocarbons found in the atmosphere. This lack of data prevents us from calculating the effect of oceanic degradation processes on the lifetimes and budgets of many trace gases. Accounting for the oceanic uptake of CH_3Cl and OCS resulted in reductions of 3% and 25% in the total atmospheric lifetimes for these species.

5.4. GC Measurements at Two Tall Towers in the U.S.

Automated, four-channel GCs have been in operation at the 610 m WITN tower in eastern North Carolina (NC) since November 1994 and at the 447-m WLEF tower in northern Wisconsin (WI) since June 1996. Every hour these instruments measure 12 trace gases (CFC-11, CFC-12, CFC-113, CH_3CCl_3, CCl_4, $CHCl_3$, C_2Cl_4, N_2O, SF_6, H_2, CH_4, and CO) at 51, 123, and 496 m above ground on the NC tower and at 30, 76, and 396 m on the WI tower. The GCs are calibrated hourly with two standards of dried, whole air stored in Aculife-treated aluminum cylinders, one of which has been diluted by 10% with zero air. The design and operation of the GC at the NC tower were described previously [*Elkins et al.*, 1996a; *Hurst et al.*, 1997a].

Trace gas mixing ratios at the two towers are variable on diurnal, synoptic, seasonal, and longer time scales. Diurnal variations result primarily from the daily development of the planetary boundary layer (PBL), which defines the mixing depth of ground-based source emissions. At night, local and regional emissions augment mixing ratios beneath a shallow (100-200 m) inversion and create significant vertical gradients. During the late morning and afternoon, this vertical structure disappears as emissions are rapidly mixed into a 1-2 km deep PBL by convection [*Hurst et al.*, 1997a, 1998]. Diurnal variability at the lower two sampling levels on each tower is greater than at the top because the nocturnal inversion consistently lies between the middle and top sampling levels.

Synoptic-scale variability is driven predominantly by the transport of pollution plumes from regional urban centers to the measurement sites. Daily mean mixing ratios (and daily standard deviations) at 496 m on the NC tower during 1996-1997 illustrate day-to-day (and diurnal-scale) variability (Figure 5.35). Daily means 5-10% above the majority of the data are regular features, especially for C_2Cl_4. Significant long-term trends in CH_3CCl_3 and SF_6 mixing ratios at the NC tower are also evident (Figure 5.35). Linear fits to regional "background" mixing ratios during 1996-1997 at the NC tower imply trends of -16.5 $\pm$ 0.5 ppt yr^{-1} for CH_3CCl_3 and 0.24 $\pm$ 0.01 ppt yr^{-1} for SF_6 [*Hurst et al.*, 1997b] which are in good agreement with background trends at remote northern hemispheric sites (Figure 5.4) [*Montzka et al.*, 1996; *Geller et al.*, 1997].

Synoptic-scale variability of trace gases at the NC tower was analyzed to identify regional-scale emission ratios [*Bakwin et al.*, 1997]. C_2Cl_4 was chosen as the reference compound because of its high ratio of atmospheric variability to measurement precision at the NC tower and its reasonably well-known emissions [*McCulloch and Midgley*, 1996]. Several statistical approaches were used for the analysis, including a method where "scores" for each trace gas were computed as the sum of its mixing ratios during pollution events >4 hours in duration. For December 1994 through August 1996, 211 pollution events of 4 to 273 hours duration were identified [*Bakwin et al.*, 1997]. Event scores for each trace gas were plotted against those for C_2Cl_4 and fit with a linear, orthogonal distance regression (Figure 5.36) to determine a regional-scale emission ratio. C_2Cl_4 correlated well with CFC-12, -11, CH_3CCl_3, SF_6, and several other gases ($r > 0.85$). North American source strengths estimated from this "score" method and a time-domain analysis of the data are in good agreement with industry estimates for $CH_3CCl_3$and CO but are 35-75% lower for CFCs. Discordance in CFC estimates may indicate that CFC emissions from the region surrounding the NC tower are not representative of North America (although CH_3CCl_3 and CO emissions appear to be) or that industry estimates of CFC emissions during 1995-1996 are too high. The latter scenario is supported by *Elkins et al.* [1993] and *Cunnold et al.* [1997] who demonstrated that global-scale observations of CFC-11 and CFC-12 mixing ratios during the 1990s are significantly lower than those calculated from emission inventories.

The synoptic-scale variability of several halogenated trace gases recently decreased at both the NC and WI towers reflecting reductions in regional-scale emissions [*Hurst et al.*, 1998]. Mixing ratio variability at all sampling heights on the towers was examined, but trends were deduced using only nighttime data from the top sampling level of each tower. This was done to minimize the influences of local sources and diurnal-scale variability, leaving regional emissions as the primary source of variability. Monthly variability, calculated as one standard deviation of monthly-binned mixing ratios with measurement errors subtracted in quadrature, was plotted as a

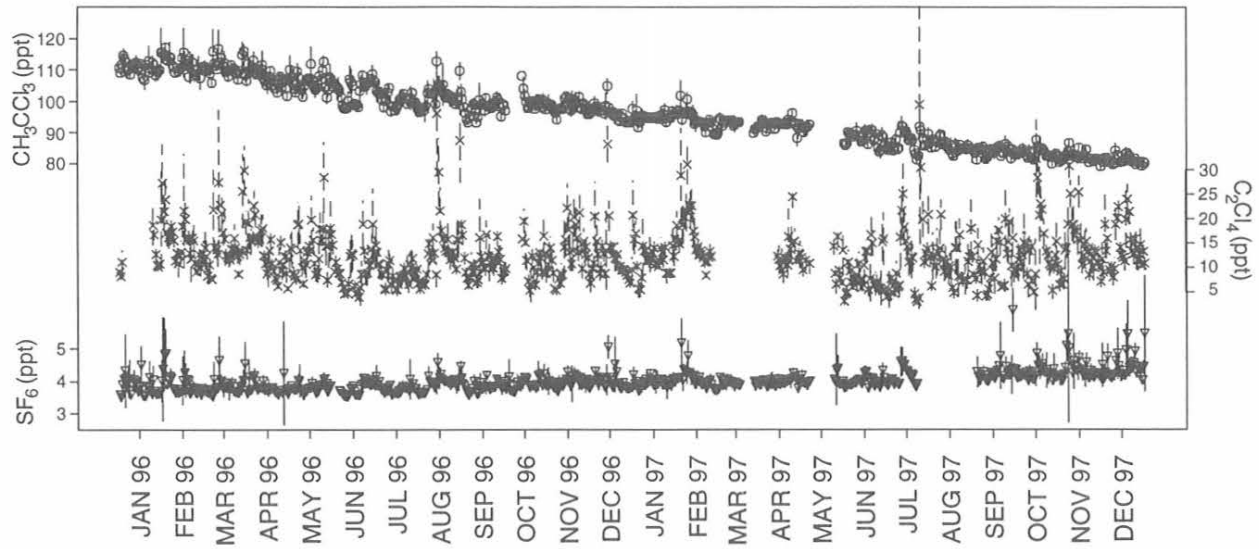

Fig. 5.35. Time series of daily mean mixing ratios of CH_3CCl_3 (circles), C_2Cl_4 (crosses), and SF_6 (inverted triangles) at the NC tower during 1996-1997. The mean mixing ratio ± one standard deviation for each day are represented by vertical bars (solid for CH_3CCl_3 and SF_6, dashed for C_2Cl_4).

time series and fit with a linear least-squares regression (Figure 5.37). Variability at the remotely-located WI tower was generally lower than at the NC tower, which is closer to large urban centers.

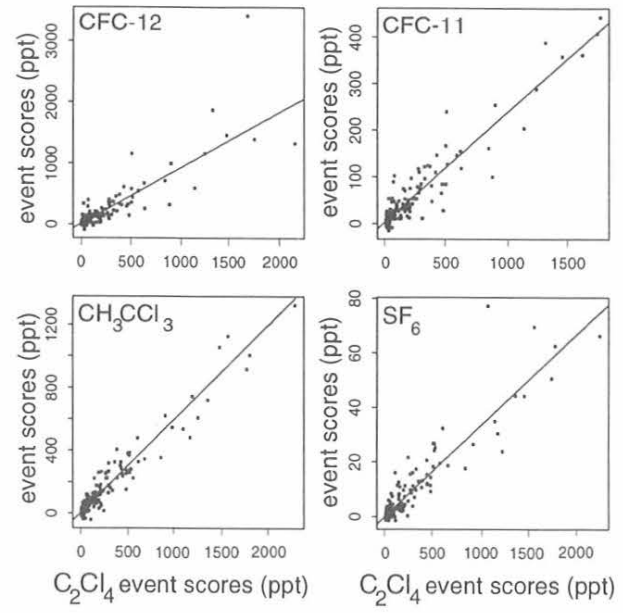

Fig. 5.36. Pollution event scores for CFC-12, CFC-11, CH_3CCl_3, and SF_6 versus scores of C_2Cl_4 at the North Carolina tower for December 1994 through August 1996. The y-axis of each panel represents event scores of the compound listed in the panel. The x-axes are scores for C_2Cl_4. Slopes of lines fit to each panel using an orthogonal distance regression reflect regional-scale emission ratios of the y-axis compound to C_2Cl_4 [from *Bakwin et al.*, 1997].

Significant decreases in the synoptic-scale variability of CFC-12, CFC-113, CH_3CCl_3, and C_2Cl_4 were observed at both towers (Table 5.10). With the exception of CH_3CCl_3, variability trends at the two towers agreed to within their quoted uncertainties. The variability trend for CH_3CCl_3 at the NC tower, -1.31 ± 0.19 ppt yr^{-1}, represents a 72 ± 11% decrease in regional emissions between early 1995 and late 1997. Trends for CFC-11, CCl_4, and SF_6 at both towers did not differ significantly from zero. However, because of the low ratios of atmospheric variability to measurement precision for these gases, only trends >25% over the entire measurement period at each tower could have been detected at a 75% level of confidence. Reductions in CFC-12, CFC-113, and CH_3CCl_3 emissions are attributed to production restrictions imposed by the Montreal Protocol. Reduced emissions of C_2Cl_4 are probably the result of recent requests to industry by the U.S. Environmental Protection Agency (EPA) to voluntarily reduce emissions of this compound because of its toxicity.

5.5. Firn Air Measurements

Past success in analyzing for halocarbons in air samples collected from firn (unconsolidated snow) at the South Pole [*Elkins et al.*, 1996a] prompted us to continue these investigations in Greenland and Antarctica. Our initial measurements of South Pole firn air were from low pressure glass flasks used in collecting air for carbon-cycle gases. Although these measurements seemed reasonable and the samples generally uncontaminated, they could only be run on two of our instruments; GC MS measurements were precluded for the South Pole samples because of a lack of available air. In April 1996 we assisted in the collection of samples from two holes at Tunu, Greenland (78°01'N, 33°59'E) and filled our usual 2.5-L stainless steel flasks to 375 kPa (yielding about 9 L of air) in

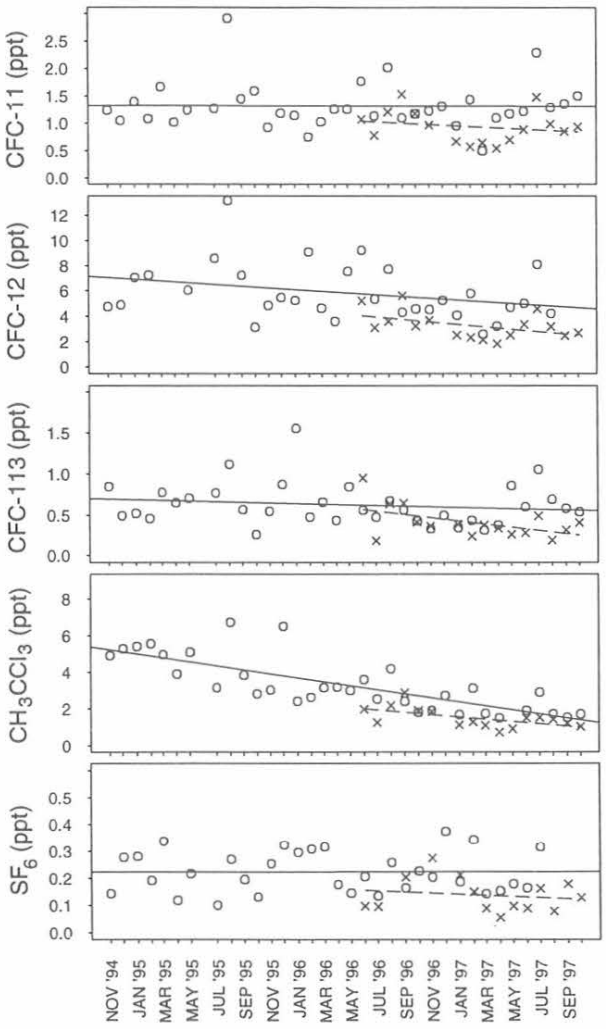

Fig. 5.37. Trends in monthly nighttime variability at the top sampling level of the North Carolina (NC) tower (circles) and Wisconsin (WI) tower (crosses). Variability was calculated as one standard deviation of nighttime mixing ratios during each month with random measurement noise removed. Lines fit to variability time series at the NC (solid) and WI (dashed) towers with least-squares regressions reflect trends in regional-scale emissions [*Hurst et al.*, 1998].

TABLE 5.10. Trends in Nighttime Atmospheric Variability at the Top Sampling Levels of Tall Towers in North Carolina and Wisconsin

Compound	Trend Slope	Slope Error	Level of Confidence
NC Tower (November 1994 – October 1997)			
CFC-11	-0.09	0.13	
CFC-12	-0.82	0.48	90%
CFC-113	-0.09	0.08	76%
CH_3CCl_3	-1.31	0.19	99%
CCl_4	0.00	0.06	
C_2Cl_4	-0.63	0.38	89%
SF_6	0.00	0.02	
WI Tower (June 1996 – October 1997)			
CFC-11	-0.15	0.18	
CFC-12	-1.15	0.60	92%
CFC-113	-0.23	0.10	95%
CH_3CCl_3	-0.75	0.28	98%
CCl_4	-0.01	0.05	
C_2Cl_4	-1.19	0.73	87%
SF_6	-0.02	0.04	

addition to the glass flasks (150 kPa, yielding only 3.8 L air, most of which is used in analyses for carbon-cycle gases by the CMDL Carbon Cycle Group). Samples were returned to Boulder for analysis on all four instruments used in flask analyses (Table 5.2). Both glass flasks and steel flasks were run on the two GC/ECD systems and steel flasks were run on the two GC/MS systems. Similarly we obtained samples in both steel and glass flasks from deep and shallow holes drilled at Siple Dome, Antarctica (81°40'S, 148°49'W), in December 1996.

Data from these sites showed that CFCs, CH_3CCl_3, CCl_4, SF_6, halons, and HCFCs were essentially absent in the early 20th century atmosphere (Figures 5.38, 5.39, and 5.40). This is not surprising information, but these samples, which, unlike the initial South Pole samples, were collected in such a way as to avoid low-level contamination of halocarbons, are the first verification of levels of CFCs and the major chlorocarbons that do not differ significantly from zero. The data demonstrate that if natural sources of these gases do exist, they are insignificant.

Results for methyl halides were more ambiguous, although it still may be possible to derive 20th century atmospheric histories for them (Figure 5.39b and Figure 5.41). Methyl chloride in the diffusive zone is about 10% higher than it is at the bottom of the profiles suggesting that activities over the past century have elevated the mixing ratio of this gas in the atmosphere by about 50 ppt. Also, in the upper 10-12 m of the firn, CH_3Cl concentrations actually decrease toward the surface by about 30 ppt. This is consistent with seasonal cycles of CH_3Cl which are associated with photochemical cycles of tropospheric OH.

Data for CH_3Br from Siple Dome agreed well with those from the South Pole, both suggesting that atmospheric CH_3Br in the earlier part of this century was about 25% lower than it is today (Figure 5.41a). However, at Tunu, Greenland, a warmer and more coastally influenced site, CH_3Br was high near the bottom of the profile, reaching mixing ratios of nearly 50 ppt at the firn-ice transition (Figure 5.41b). Tests confirm that this elevation in concentration at depth is not an artifact of sample collection, storage, or analysis. This leads us to believe that the observed high values for CH_3Br in the firn at Tunu are real, although not necessarily of atmospheric origin. (This feature was also observed at Tunu for at least one other marine biogenic gas, CH_3I, and it was observed for $CHBr_3$ at Siple Dome where CH_3Br and CH_3I do not appear to have been produced.) A model of the

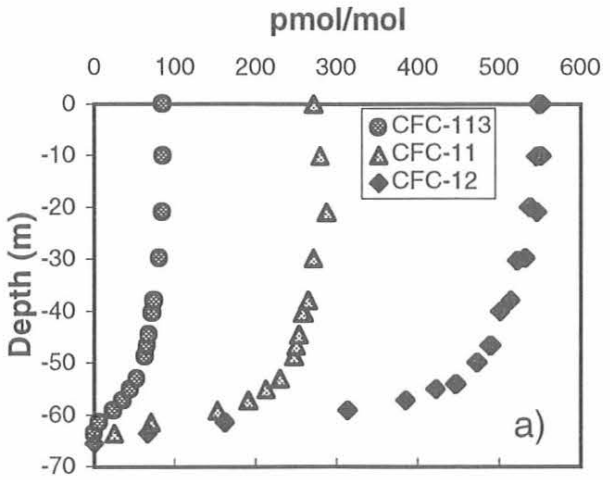

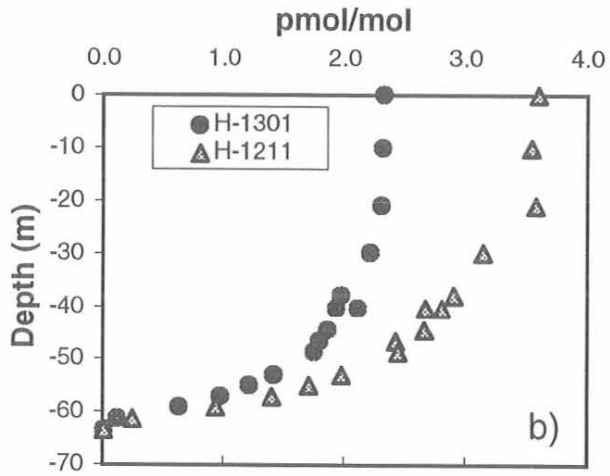

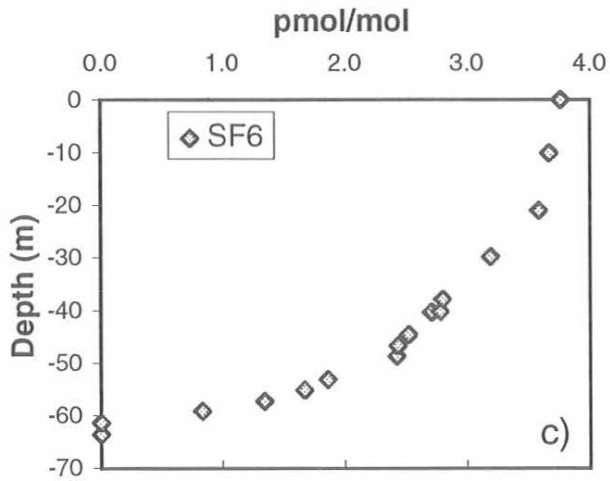

Fig. 5.38. "Conservative" gases of anthropogenic origin in Tunu firn air. (a) CFC's, (b) halons, (c) SF_6. CO_2 in air at the bottom of the Tunu, Greenland, profile corresponds to atmospheric CO_2 in the early 1930s.

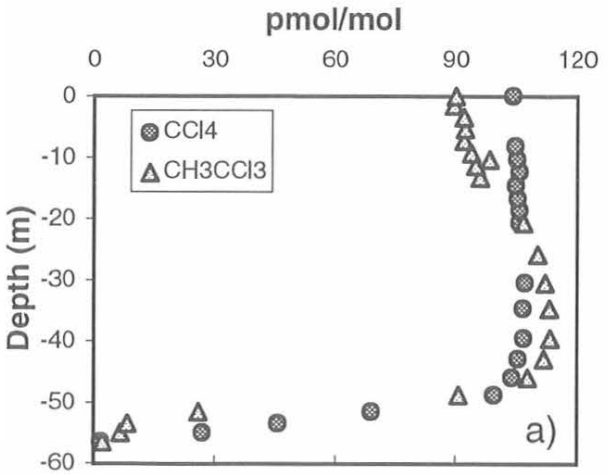

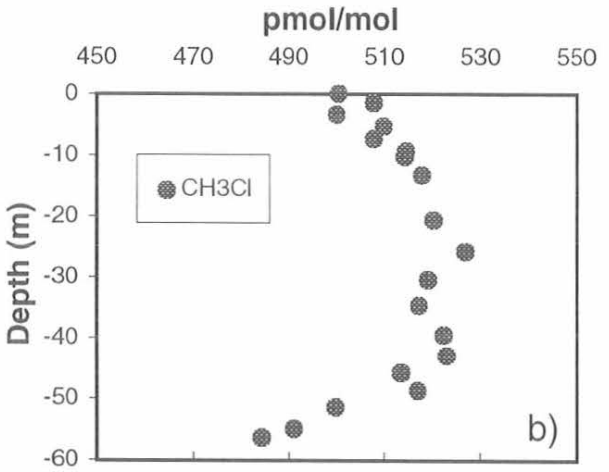

Fig. 5.39. Chlorocarbons in Siple Dome firn air. (a) CH_3CCl_3 and CCl_4, (b) CH_3Cl. CO_2 in air at the bottom of the Siple Dome profile corresponds to atmospheric CO_2 in the early 1950s.

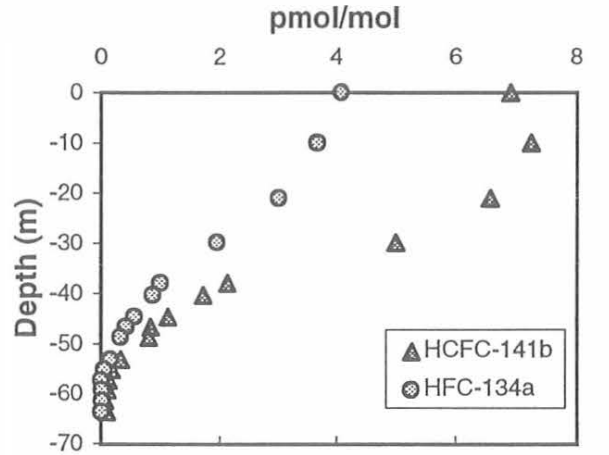

Fig. 5.40. Replacement compounds for CFCs in Tunu firn air.

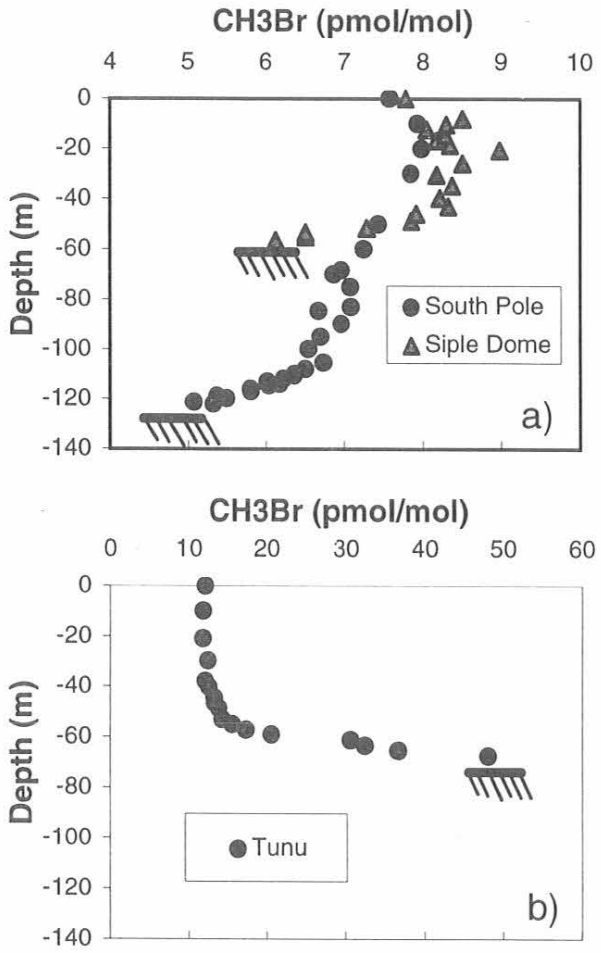

Fig. 5.41. Methyl bromide in firn air. (a) Antarctica, (b) Tunu, Greenland.

firn profiles strongly suggests that CH_3Br is produced near the firn-ice transition, a process that could not have been happening at South Pole or Siple Dome and yield the observed profiles.

Processes in the upper 10 m of firn also may affect CH_3Br concentrations. At each antarctic site, the CH_3Br concentration was elevated by as much as 1 ppt (10-15%) in samples just below the surface. This feature was consistent, though at present unexplained. Such variations did not appear throughout the profiles which suggests this may be a phenomenon limited to the upper 10 m. How this affects the overall profile is difficult to ascertain without first understanding the process. All firn samplings were conducted during the summer months thus precluding any evaluation of seasonal effects in the surface. In the fall of 1997, flasks were sent to SPO for sampling from a 15 m deep hole in winter and summer of 1998.

5.5. REFERENCES

Anbar, A.D., Y.L. Yung, and F.P. Chavez, Methyl bromide: Ocean sources, ocean sinks, and climate sensitivity, *Global Biogeochem. Cycles, 10(1)*, 175-190, 1996.

Bakwin, P.S., D.F. Hurst, P.P. Tans, and J.W. Elkins, Anthropogenic sources of halocarbons, sulfur hexafluoride, carbon monoxide, and methane in the southeastern United States, *J. Geophys. Res., 102*, 15,915-15,925, 1997.

Battle, M., M. Bender, T. Sowers, P. Tans, J. Butler, J. Elkins, J. Ellis, T. Conway, N. Zhang, P. Lang, and A. Clarke, Histories of atmospheric gases from the firn at South Pole, *Nature, 383*, 231-235, 1996.

Bouwman, A.F., K.W. Van der Hoek, and J.G.J. Olivier, Uncertainties in the global source distribution of nitrous oxide, *J. Geophys. Res., 100(D2)*, 2785-2800, 1995.

Butler, J.H., J.W. Elkins, T.M. Thompson, B.D. Hall, T.H. Swanson, and V. Koropalov, Oceanic consumption of CH_3CCl_3: Implications for tropospheric OH, *J. Geophys. Res., 96*, 22,347-22,355, 1991.

Butler, J.H., The potential role of the ocean in regulating atmospheric CH_3Br, *Geophys. Res. Lett., 21*, 185-188, 1994.

Butler, J.H., J.M. Lobert, S.A., Yvon, and L.S. Geller, The distribution and cycling of halogenated trace gases between the atmosphere and ocean, in *The Expedition ANTARKTIS XII of RV Polarstern in 1994/95, Reports of Legs ANT XII/1 and 2*, pp. 27-40, Alfred Wegener Insitut fur Polar und Meeresforschung, Bremerhaven, Germany, 1995.

Butler, J.H., S.A. Montzka, A.D. Clarke, J.M. Lobert, and J.W. Elkins, Growth and distribution of halons in the atmosphere, *J. Geophys. Res., 103(D1)*, 1503-1511, 1998.

Chen, L., Y. Makide, and T. Tominaga, Distribution and trend of chlorodifluoromethane (HCFC-22) in the atmosphere, *Chem. Lett., 12*, 2423-2426, 1994.

Chin, M., and D.D. Davis, A reanalysis of carbonyl sulfide as a source of stratospheric background sulfur aerosol, *J. Geophys. Res., 100*, 8993-9005, 1995.

Cicerone, R., Analysis of sources and sinks of atmospheric nitrous oxide (N_2O), *J. Geophys. Res., 94*, 18,265-18,271, 1989.

Cunnold, D.M., R.F. Weiss, R.G. Prinn, D. Hartley, P.G. Simmonds, P.J. Fraser, B.R. Miller, F.N. Alyea, and L. Porter, GAGE/AGAGE measurements indicating reductions in global emissions of CCl_3F and CCl_2F_2 in 1992-1994, *J. Geophys. Res., 102*, 1259-1269, 1997.

Daniel, J.S., S.M. Schauffler, W.H. Pollock, S. Solomon, A. Weaver, L.E. Heidt, R.R. Garcia, E.L. Atlas, and J.F. Vedder, On the age of stratospheric air and inorganic chlorine and bromine release, *J. Geophys. Res., 101(D11)*, 16,757-16,770, 1996.

DeBruyn W.J., and E.S. Saltzman, Diffusivity of methyl bromide in water, *Mar. Chem., 57*, 55-59, 1997a.

DeBruyn W.J., and E.S. Saltzman, The solubility of methyl bromide in pure water, 35‰ sodium chloride and seawater, *Mar. Chem., 56*, 51-57, 1997b.

Ehhalt, D.H., P.J. Fraser, D. Albritton, R.J. Cicerone, M.A.K. Khalil, M. Legrand, Y. Makide, F.S. Rowland, L.P. Steele, and R. Zander, Trends in source gases, in *Report of the International Ozone Trends Panel, 1988*, World Meteorological Organization, Geneva, 1988.

Elkins, J.W., T.M. Thompson, T.H. Swanson, J.H. Butler, B.D. Hall, S.O. Cummings, D.A. Fisher, and A.G. Raffo, Slowdown in the growth rates of atmospheric chlorofluorocarbons 11 and 12, *Nature, 364*, 780-783, 1993.

Elkins, J.W., J.H. Butler, T.M. Thompson, S.A. Montzka, R.C. Myers, J.M. Lobert, S. Yvon, P.R. Wamsley, F.L. Moore, J.M. Gilligan, D.F. Hurst, A.D. Clarke, T.H. Swanson, C.M. Volk, L.T. Lock, L.S. Geller, G.S. Dutton, R.M. Dunn, M.F. Dicorelto, T.J. Baring, and A.H. Hayden, 5. Nitrous Oxide and Halocompounds,

Climate Monitoring and Diagnostics Laboratory No. 23 Summary Report 1994-1995, D.J. Hofmann, J.T. Peterson, and R. Rosson (eds.), 84-111, NOAA Env. Res. Labs., Boulder, CO, 1996a.

Elkins, J.W., D.W. Fahey, J. M. Gilligan, G.S. Dutton, T.J. Baring, C.M. Volk, R.E. Dunn, R.C. Myers, S.A. Montzka, P.R. Wamsley, A.H. Hayden, J.H. Butler, T.M. Thompson, T.H. Swanson, E.J. Dlugokencky, P.C. Novelli, D.F. Hurst, J.M. Lobert, S.J. Ciciora, R.J. McLaughlin, T.L. Thompson, R.H. Winkler, P.J. Fraser, L.P. Steele and M.P. Lucarelli, Airborne gas chromatograph for in situ measurements of long-lived species in the upper troposphere and lower stratosphere, *Geophys. Res. Lett., 23(4)*, 347-350, 1996b.

Elliott, S., E. Lu, and F.S. Rowland, Rates and mechanisms for the hydrolysis of carbonyl sulfide in natural waters, *Environ. Sci. Technol., 23*, 458-461, 1989.

Fabian, P., R. Borchers, and K. Kourtidis, Bromine-containing source gases during EASOE, *Geophys. Res. Lett., 21(13)*, 1219-1222, 1994.

Fabian, P., R. Borchers, R. Leifer, B.H. Subbaraya, S. Lal, and M. Boy, Global stratospheric distribution of halocarbons, *Atmos. Environ., 30*, 1787-1796, 1996.

Geller, L.S., J.W. Elkins, J.M. Lobert, A.D. Clarke, D.F. Hurst, J.H. Butler, and R.C. Myers, Tropospheric SF_6: Observed latitudinal distribution and trends, derived emissions and interhemispheric exchange time, *Geophys. Res. Lett., 24(6)*, 675-678, 1997.

Gerkins, R.R., and J.A. Franklin, The rate of degradation of 1,1,1-trichloroethane in water by hydrolysis and dehydrohalogenation, *Chemosphere, 19*, 1929-1937, 1989.

Gossett, J.M., Measurement of Henry's Law constants for C_1 and C_2 chlorinated hydrocarbons, *Environ. Sci. Technol., 21(2)*, 202-208, 1987.

Hall, T.M., and R.A. Plumb, Age as a diagnostic of stratospheric transport, *J. Geophys. Res., 99*, 1059-1070, 1994.

Hurst, D.F., P.S. Bakwin, R.C. Myers, and J.W. Elkins, Behavior of trace gas mixing ratios on a very tall tower in North Carolina, *J. Geophys. Res., 102*, 8825-8835, 1997a.

Hurst, D.F., P.S. Bakwin,, and J.W. Elkins, Recent trends in halogenated trace gas mixing ratios and variance on two tall towers in the United States, *EOS Trans. AGU, 78*, Fall Meet. Suppl., F94, 1997b.

Hurst, D.F., P.S. Bakwin, and J.W. Elkins, Recent trends in the variability of halogenated trace gases over the United States, *J. Geophys. Res., 103(D19)*, 25,299-25,306, 1998.

Intergovernmental Panel on Climate Change (IPCC), Climate Change 1994: Radiative Forcing of Climate Change and An Evaluation of the IPCC IS92 Emission Scenarios, Intergovernmental Panel on Climate Change, J.T. Houghton, L.G.M. Filho, J. Bruce, H. Lee, B.A. Callander, E. Haites, N. Harris, and K. Maskell (eds.), 339 pp., Cambridge, UK, 1995.

Jeffers, P.M., L.M. Ward, L.M. Woytowitch, and N.L. Wolfe, Homogeneous hydrolysis rate constant for selected chlorinated methanes, ethanes, ethenes, and propanes, *Environ. Sci. Technol., 23*, 965-969, 1989.

Johnson, J.E., and H. Harrison, Carbonyl sulfide concentrations in the surface waters and above the Pacific Ocean, *J. Geophys. Res., 91*, 7883-7888, 1986.

Kaye, J.A., S.A. Penkett, and F.M. Ormond, Report on concentrations, lifetimes and trends of CFCs, halons and related species, *NASA RP 1339*, 248 pp., 1994.

Kaye, J.A., S.A. Penkett, F.M. Ormond, P. Fraser, D. Fisher, P. Bloomfield, S.P. Sander, and M.K.W. Ko, *Report on concentrations, lifetimes and trends of CFCs, halons and related species*, NASA, Washington, DC, 1994.

Khalil, M.A.K., and R.A. Rasmussen, Constraints imposed by the ice core data on the budgets of nitrous oxide and methane, in *28th Liege International Astrophysical Colloquium June 26-30, 1989*, edited by P.J. Crutzen, J.C. Gerard, and R. Zander, pp. 403-410, University de Liege, Liege, Belgium, 1989.

Khalil, M.A.K., and R.A. Rasmussen, Trace gases over Antarctica: Bromine, chlorine, and organic compounds involved in global change, *Ant. J. U. S., 27(5)*, 267-269, 1992.

Khalil, M.A.K., R.A. Rasmussen, and R. Gunawardena, Atmospheric methyl bromide: Trends and global mass balance, *J. Geophys. Res., 98(D2)*, 2887-2896, 1993.

Kim, K.-R., and H. Craig, Nitrogen-15 and oxygen-18 characteristics of nitrous oxide: A global perspective, *Science, 262*, 1855-1857, 1993.

King, D.B., and E.S. Saltzman, Removal of methyl bromide in coastal seawater: Chemical and biological rates, *J. Geophys. Res., 102*, 18,715-18,721, 1997.

Lal, S., R. Borchers, P. Fabian, P.K. Patra, and B.H. Subbaraya, Vertical distribution of methyl bromide over Hyderbad, India, *Tellus, 46B*, 373-377, 1994.

Leuenberger, M., and U. Siegenthaler, Ice-age atmospheric concentration of nitrous oxide from an Antarctic ice core, *Nature, 360*, 449-451, 1992.

Li, Y.H., T.H. Peng, W.S. Broecker, and H.G. Ostlund, The average vertical mixing coefficient for the oceanic thermocline, *Tellus, 36B*, 212-217, 1984.

Liss, P.S., and L. Merlivat, Air-sea gas exchange rates: Introduction and synthesis, in *The Role of Air-Sea Exchange in Geochemical Cycling*, edited by P. Buat-Menard, pp. 113-127, D. Reidel, Norwell, MA, 1986.

Lobert J.M., J.H. Butler, S.A. Montzka, L.S. Geller, R.C. Myers, and J.W. Elkins, A net sink for atmospheric CH_3Br in the East Pacific Ocean, *Science, 267*, 1002-1005, 1995.

Lobert, J.M., S.A. YvonLewis, J.H. Butler, S.A. Montzka, and R.C. Myers, Undersaturation of CH_3Br in the Southern Ocean, *Geophys. Res. Lett., 24(2)*, 171-172, 1997.

Lobert, J.M., J.H. Butler, L.S. Geller, S.A. Yvon, S.A. Montzka, R.C. Myers, A.D. Clarke, and J.W. Elkins, Blast 94: Bromine Latitudinal Air/Sea Transect, 1994, Report on Oceanic Measurements of Methyl Bromide and Other Compounds, *NOAA Tech. Memo. ERL CMDL-10*, Environmental Research Laboratories, Boulder, CO, 1996.

Loewenstein, M., J.R. Podolske, K.R. Chan, and S.E. Strahan, Nitrous oxide as a dynamical tracer in the 1987 Airborne Antarctic Ozone Experiment, *J. Geophys. Res., 94(D9)*, 11,589-11,598, 1989.

Lorenzen-Schmidt, H., Untersuchungen zur atmosphaerischen Verteilung un zum photochemischen Abbau leichtfluechtiger Bromverbindungen, Ph.D., Alfred Wegener Institute fuer Polar-und Meeresforschung, Bremerhaven, 1994.

Machida, T., T. Nakazawa, Y. Fujii, S. Aoki, and O. Watanabe, Increase in the atmospheric nitrous oxide concentration during the last 250 years, *Geophys. Res. Lett., 22(21)*, 2921-2924, 1995.

Maiss, M., and I. Levin, Global increase of SF_6 observed in the atmosphere, *Geophys. Res. Lett., 21(7)*, 569-572, 1994.

McCulloch, A., and P.M. Midgley, The production and global distribution of emissions of trichloroethene, tetrachloroethene, and dichloromethane over the period 1988-1992, *Atmos. Environ., 30*, 601-608, 1996.

McLinden, M.O., Physical properties of alternatives to the fully halogenated chlorofluorocarbons, in *Scientific Assessment of Stratospheric Ozone: 1989 Vol. II Appendix AFEAS Report*, WMO Global Ozone Research and Monitoring Project-Report No. 20, 469 pp., 1989.

Moelwyn-Hughes, E.A., The hydrolysis of methyl halides, *Proc. Roy. Soc. A, 164*, 295-306, 1938.

Montzka, S.A., J.H. Butler, R.C. Myers, T.M. Thompson, T.H. Swanson, A.D. Clarke, L.T. Lock, and J.W. Elkins, Decline in the tropospheric abundance of halogen from halocarbons: Implications for stratospheric ozone depletion, *Science, 272*, 1318-1322, 1996.

Moore, R.M., C.E. Green, and V.K. Tait, Determination of Henry's Law constants for a suite of naturally occurring halogenated methanes in seawater, *Chemosphere*, 30, 1183-1191, 1995.

Oertel, T., Verteilung leichtfluechtiger organobromver-bindungen in der marinen troposphaere un im oberflaechenwasser des Atlantiks, PhD., Universität Bremen, Germany, 1992.

Oort, A.H., and J.J. Yienger, Observed interannual variability in the Hadley circulation and its connection to ENSO, *J. Clim., 9*, 2751-2767, 1996.

Pilinis, C., D.B. King, and E.S. Saltzman, The oceans: A source or a sink of methyl bromide? *Geophys. Res. Lett., 23(8)*, 817-820, 1996.

Plumb, R.A., A "tropical pipe" model of stratospheric transport, *J. Geophys. Res., 101*, 3957-3972, 1996.

Plumb, R.A., and M.K.W. Ko, Interrelationships between mixing ratios of long-lived stratospheric constituents, *J. Geophys. Res., 97*, 10,145-10,156, 1992.

Prinn, R.G., R.F. Weiss, B.R. Miller, J. Huang, F.N. Alyea, D.M. Cunnold, P.B. Fraser, D.E. Hartley, and P.G. Simmons, Atmospheric trends and lifetime of trichloroethane and global average hydroxyl radical concentrations based on 1978-1994 ALE/GAGE measurements, *Science*, 269, 187-192, 1995.

Ravishankara, A.R., S. Solomon, A.A. Turnipseed, and R.F. Warren, Atmospheric lifetimes of long-lived halogenated species, *Science, 259*, 194-200, 1993.

Schauffler, S.M., L.E. Heidt, W.H. Pollock, T.M. Gilpin, J.F. Vedder, S. Solomon, R.A. Lueb, and E.L. Atlas, Measurements of halogenated organic compounds near the tropical tropopause. *Geophys. Res. Lett., 20(22)*, 2567-2570, 1993.

Schimel, D., D. Alves, I. Enting, M. Heimann, F. Joos, D. Raynaud, T. Wigley, M. Prather, R. Derwent, D. Ehhalt, P. Fraser, E. Sanhueza, X. Zhou, P. Jonas, R. Charlson, H. Rodhe, S. Sadasivan, K.P. Shine, Y. Fouquart, V. Ramaswamy, S. Solomon, J. Srinivasan, D. Albritton, R. Derwent, I. Isaksen, M. Lal, and D. Wuebbles, Radiative Forcing of Climate Change, in *Climate Change 1995: The Science of Climate Change*, edited by J.T. Houghton, L.G. Meira Filho, B.A. Callander, N. Harris, A. Kattenberg, and K. Maskell, pp. 65-131, Cambridge Univ. Press, U.K., 1996.

Singh, O.N., R. Borchers, P. Fabian, S. Lal, and B.H. Subbaraya, Measurements of atmospheric BrOx radicals in the tropical and mid-latitude atmosphere, *Nature, 334*, 593-595, 1988.

Singh, H.B., and M. Kanakidou, An investigation of the atmospheric sources and sinks of methyl bromide, *Geophys. Res. Lett., 20(2)*, 133-136, 1993.

Singh, H.B., L.J. Salas, and R.E. Stiles, Methyl halides in and over the eastern Pacific (40°N-32°S), *J. Geophys. Res., 88*, 3684-3690, 1983.

Thompson, T.M., W.D. Komhyr, and E.G. Dutton, Chlorofluorocarbon-11, -12, and nitrous oxide measurements at the NOAA/GMCC baseline stations (16 September 1973 to 31 December 1979), in *NOAA Tech. Rep. ERL 428-ARL 8*, 124 pp., NOAA Env. Res. Labs., Boulder, CO, 1985.

Ulshöfer, V.S. and M.O. Andreae, Carbonyl sulfide (COS) in the surface ocean and the atmospheric COS budget, *Aquat. Geochem.*, submitted, 1997.

United Nations Environmental Programme (UNEP), *Montreal Protocol on Substances that Deplete the Ozone Layer, Final Act*, 15 pp., United Nations Environmental Programme, Nairobi, 1987.

United Nations Environmental Programme (UNEP), Report of the Ninth Meeting of the Parties to the Montreal Protocol on Substances that Deplete the Ozone Layer (Montreal), United Nations Environmental Programme, New York, 1997.

Volk, C.M., J.W. Elkins, D.W. Fahey, R.J. Salawitch, G.S. Dutton, J.M. Gilligan, M.H. Profitt, M. Loewenstein, J.R. Podolske, K. Minschwaner, J.J. Margitan, and K.R. Chan, Quantifying transport between the tropical and mid-latitude lower stratosphere, *Science, 272*, 1763-1768, 1996.

Volk, C.M., J.W. Elkins, D.W. Fahey, G.S. Dutton, J.M. Gilligan, M. Loewenstein, J.R. Podolske, K.R. Chan and M.R. Gunson, Evaluation of source gas lifetime from stratospheric observations, *J. Geophys. Res., 102(D21)* , 25,543-25,564, 1997.

Wamsley, P.R., J.W. Elkins, D.W. Fahey, G.S. Dutton, C.M. Volk, R.C. Myers, S.A. Montzka, J.H. Butler, A.D. Clarke, P.J. Fraser, L.P. Steele, M.P. Lucarelli, E.L. Atlas, S.M. Schauffler, D. R. Blake, F.S. Rowland, W.T. Sturges, J.M. Lee, S.A. Penkett, A. Engel, R.M. Stimpfle, K.R. Chan, D.K. Weisenstein, M.K.W. Ko and R.J. Salawitch, Distribution of halon-1211 in the upper troposphere and lower stratosphere and the 1994 total bromine budget, *J. Geophys. Res., 103(D1)*, 1513-1526, 1998.

Wang, C. J-L., D.R. Blake, and F.S. Rowland, Seasonal variations in the atmospheric distribution of a reactive chlorine compound, tetrachloroethene (CCl2=CCl2), *Geophys. Res. Lett.*, 22, 1097-1100, 1995.

Wanninkhof, R., Relationship between wind speed and gas exchange over the ocean, *J. Geophys. Res., 97*, 7373-7382, 1992.

Wilke, C.R., and P. Chang, Correlation of diffusion coefficients in dilute solutions, *AIChE. J., 35*, 281-289, 1955.

Wine, P.H., and W.L. Chameides, Possible atmospheric lifetimes and chemical reaction mechanisms for selected HCFCs, HFCs, CH_3CCl_3, and their degradation products against dissolution and/or degradation in seawater and cloudwater, in *Scientific Assessment of Stratospheric Ozone: 1989 Vol. II Appendix AFEAS Report*, WMO Global Ozone Research and Monitoring Project-Report No. 20, 469 pp., 1989.

Woodbridge, E.L., J.W. Elkins, D.W. Fahey, L.E. Heidt, S. Solomon, T.J. Baring, T.M. Gilpin, W.H. Pollock, S.M. Schauffler, E.L. Atlas, M. Loewenstein, J.R. Podolske, C.R. Webster, R.D. May, J.M. Gilligan, S.A. Montzka, K.A. Boering and R.J. Salawitch, Estimates of total organic and inorganic chlorine in the lower stratosphere from in situ and flask measurements, *J. Geophys. Res., 100(D2)*, 3057-3064, 1995.

World Meteorological Organization (WMO), *Scientific Assessment of Ozone Depletion: 1991, Global Ozone Research and Monitoring Project, 25*, 357, WMO Geneva, 1992.

World Meteorological Organization (WMO), *Scientific Assessment of Ozone Depletion: 1994, Global Ozone Research and Monitoring Project, 37*, D.L. Albritton, and R.J. Aucamp, eds., p. 451, WMO, Geneva, 1995.

Yvon, S.A., and J.H. Butler, An improved estimate of the oceanic lifetime of atmospheric CH_3Br, *Geophys. Res. Lett., 23(1)*, 53-56, 1996.

Yvon-Lewis, S.A., and J.H. Butler, The potential effect of biological degradation on the lifetime of atmospheric CH_3Br, *Geophys. Res. Lett., 24(10)*, 1227-1230, 1997.